A stable AIEgen cis-diarylethene-Based 'ESIPT' benchmark

Tingting Zhang,[a]† Liu Wen,[a]† Genjiang Liu,[a] Jiaying Yan,*[a,b] Xiang Liu,[a,c] Kaibo Zheng,[a] and Nuonuo Zhang*[a]

[a]*College of Materials and Chemical Engineering, and Key Laboratory of Inorganic Nonmetallic Crystalline and Energy Conversion Materials, China Three Gorges University, Hubei, Yichang 443002, PR China*

[b]*State Key Laboratory of Coordination Chemistry, Nanjing University, Jiangsu, Nanjing 210093, PR China*

[c]*Material Analysis and Testing Center, China Three Gorges University, Hubei, Yichang 443002, PR China*

*Corresponding authors. E-mail addresses: yanjiaying327@126.com and nnzhang2015@ctgu.edu.cn

Table of Contents

1 General Information

General

All reagents and solvents were obtained from commercial sources and used without further purification, unless otherwise noted. All chromatographic separations were carried out on silica gel (300-400 mesh). ^{1}H NMR and ^{13}C NMR spectra were recorded on Bruker 400 MHz spectrometer at 298 K. $CDCl_3$ and DMSO-d_6 was used as solvent and TMS as internal reference. The chemical shifts were reported in parts per million (δ) relative to the appropriate reference signal: residual chloroform (δ_H 7.26) or DMSO (the quintet centered at 2.50 ppm). High resolution mass spectra were measured on Bruker APCI instrument or SYNAPT G2 analysis instrument. UV–Vis spectra in various solvents were detected on Shimadzu UV-2600 in 10 mm quartz cell spectrometer. Fluorescence spectra were obtained using a Shimadzu FL-4600 spectrometer, emission wavelengths λ are reported in nm.

Quantum yield method

Relative fluorescence quantum efficiencies of compounds **NBs** in solvents were obtained by comparing the areas under the corrected emission spectrum of the test sample in various solvents with Rhodamine B (Φ_f= 0.49 in ethanol) and Fluorescein (Φ_f =0.9 in 0.1 M NaOH) for **NBs**. Non-degassed, spectroscopic grade solvents and a 10 mm quartz cuvette were used. Dilute solutions (0.01<A<0.05) were used to minimize the reabsorption effects. Quantum yields were determined using the following equation:

$$\Phi_X = \Phi_S (I_X/I_S) (A_S/A_X) (n_X/n_S)^2$$

Where Φ_S stands for the reported quantum yield of the standard, I stands for the integrated emission spectra, A stands for the absorbance at the excitation wavelength and n stands for the refractive index of the solvent being used. X subscript stands for the test sample, and S subscript stands for the standard.

Computational method

The geometries of the ground states, excited states were optimized by the density functional theory (DFT) and time-dependent density functional theory (TDDFT) method, and related optical properties of all molecules were calculated with TDDFT methodology with a B3LYP hybrid function in combination with a polarizable continuum model (PCM) in toluene. The 6-31G(d) basis set was employed for all atoms [1, 2]. To further understand the specific ESIPT process, the potential energy curves in both S0 and S1 states are scanned by constrained optimizations with fixing the length of -NH- bond. Other degrees of freedom are optimized without any constraint also using the DFT and TD-B3LYP theory with a 6-31G (d) basis set under the structures optimized at the DFT and TD-B3LYP/6-31G (d) level. All calculations of the present work are performed using Gaussian 09 program package [3].

The optimized structures of ground and excited states (N-S_0, N-S_1, T-S_1) were calculated by DFT and TDDFT methods. The potential energy curves are constructed by increasing the N-H bond length in enhancement of 0.06 Å for 12 steps using DFT/B3LYP method in the S_0 state and using TDDFT/B3LYP method in the S_1 state. The highest energy in excited state (H-S_1) was obtained in the potential energy curves.

[1] N. Zhang, T. Zhang, X. Liu, G. Liu, J. Yan and K. Zheng, Journal of Molecular Liquids, 2019, 286, 110887.

[2] W. J. Hehre, R. Ditchfield and J. A. Pople, The Journal of Chemical Physics, 1972, 56, 2257-2261.

[3] Gaussian 09, Revision A.1, Frisch, M. J.; Trucks, G. W.; Schlegel, H. B.; Scuseria, G. E.; Robb, M. A.; Cheeseman, J. R.; Scalmani, G.; Barone, V.; Mennucci, B.; Petersson, G. A.; Nakatsuji, H.; Caricato, M.; Li, X.; Hratchian, H. P.; Izmaylov, A. F.; Bloino, J.; Zheng, G.; Sonnenberg, J. L.; Hada, M.; Ehara, M.; Toyota, K.; Fukuda, R.; Hasegawa, J.; Ishida, M.; Nakajima, T.; Honda, Y.; Kitao, O.; Nakai, H.; Vreven, T.; Montgomery, Jr., J. A.; Peralta, J. E.; Ogliaro, F.; Bearpark, M.; Heyd, J. J.; Brothers, E.; Kudin, K. N.; Staroverov, V. N.; Kobayashi, R.; Normand, J.; Raghavachari, K.; Rendell, A.; Burant, J. C.; Iyengar, S. S.; Tomasi, J.; Cossi, M.; Rega, N.; Millam, N. J.; Klene, M.; Knox, J. E.; Cross, J. B.; Bakken, V.; Adamo, C.; Jaramillo, J.; Gomperts, R.; Stratmann, R. E.; Yazyev, O.; Austin, A. J.; Cammi, R.; Pomelli, C.; Ochterski, J. W.; Martin, R. L.; Morokuma, K.; Zakrzewski, V. G.; Voth, G. A.; Salvador, P.; Dannenberg, J. J.; Dapprich, S.; Daniels, A. D.; Farkas, Ö.;

Foresman, J. B.; Ortiz, J. V.; Cioslowski, J.; Fox, D. J. Gaussian, Inc., Wallingford CT, 2009

2 Procedure for the Synthesis of NBs

To a mixture of substituted 2,3,3-trimethylbenzoindole (1 mmol), 4-acetyl-2-formylpyrrole or 2-formylpyrrole (1 mmol), AcOH (86 uL, 1.5 mmol) and piperidine (0.1 mL, 1.4 mmol) in toluene (50 mL) was added and the mixture was refluxed for 4 h. The completion of reaction was confirmed by TLC. The brown dark reaction mixture was cooled, concentrated to viscous liquid and chromatographic separation. By column chromatography (silica gel, petroleum/dichloromethane 4:1 to 1:3) to give the corresponding product **NBs** as a solid.

NB-1: Orange red solid, 80 mg, yield: 22 %.; ^{1}H NMR (400 MHz, $CDCl_3$) δ 15.90 (s, 1H), 8.49 (d, *J* = 8.2 Hz, 1H), 8.02 (d, *J* = 13.0 Hz, 1H), 7.94 (d, *J* = 8.2 Hz, 1H), 7.80 (d, *J* = 8.2 Hz, 1H), 7.71 – 7.62 (m, 1H), 7.58 – 7.52 (m, 1H), 7.50 (d, *J* = 8.2 Hz, 1H), 7.18 (t, *J* = 2.6 Hz, 1H), 6.90 (t, *J* = 2.5 Hz, 1H), 6.32 (d, *J* = 13.0 Hz, 1H), 4.36 (q, *J* = 7.1 Hz, 2H), 1.47 (s, 6H), 1.41 (t, *J* = 7.1 Hz, 3H). ^{13}C NMR (101 MHz, $CDCl_3$) δ = 182.57, 165.20, 147.77, 141.69, 133.93, 133.62, 128.57, 128.27, 126.72, 126.63, 126.38, 125.88, 122.68, 119.71, 119.63, 116.95, 113.48, 112.46, 59.88, 54.62, 23.02, 14.56. HRMS (ESI) Calcd. for $C_{23}H_{23}N_2O_2$ $[M+H]^+$: 359.1754, found 358.1749.

NB-2: Orange yellow solid, 120 mg, yield: 33 %.–^{1}H NMR (400 MHz, $CDCl_3$) δ 15.76 (s, 1H), 8.46 (d, *J* = 8.3 Hz, 1H), 7.94 (d, *J* = 8.2 Hz, 1H), 7.86 – 7.82 (m, 1H), 7.79 (d, *J* = 8.2 Hz, 1H), 7.67 (dd, *J* = 11.2, 4.0 Hz, 1H), 7.59 – 7.52 (m, 1H), 7.49 (d, *J* = 8.2 Hz, 1H), 7.01 (s, 1H), 6.89 (d, *J* = 12.6 Hz, 1H), 6.12 (d, *J* = 12.6 Hz, 1H), 4.35 (q, *J* = 7.1 Hz, 2H), 1.46 (s, 6H), 1.40 (t, *J* = 7.1 Hz, 3H). ^{13}C NMR (101 MHz, $CDCl_3$) δ = 182.81, 164.80, 147.89, 141.41, 133.94, 132.06, 129.59, 128.56, 126.74, 126.40, 126.31, 125.88, 125.59, 122.64, 119.67, 118.34, 116.93, 110.16, 59.92, 54.54, 23.09, 14.58, 0.05. HRMS (ESI) Calcd. for $C_{23}H_{23}N_2O_2$ $[M+H]^+$: 359.1754, found 359.1746.

NB-3: Orange red solid, 100 mg, yield: 28 %. ^{1}H NMR (400 MHz, $CDCl_3$) δ 15.49 (s, 1H), 8.06 (d, *J* = 8.4 Hz, 1H), 8.02 (d, *J* = 13.1 Hz, 1H), 7.97 (d, *J* = 8.1 Hz, 1H), 7.89 (dd, *J* = 21.0, 8.5 Hz, 2H), 7.63 – 7.55 (m, 1H), 7.53 – 7.45 (m, 1H), 7.06 (t, *J* = 2.6 Hz, 1H), 6.85 (t, *J* = 2.6 Hz, 1H), 6.33 (d, *J* = 13.1 Hz, 1H), 4.36 (d, *J* = 7.1 Hz, 2H), 1.64 (s, 6H), 1.41 (t, *J* = 7.1 Hz, 3H). ^{13}C NMR (101 MHz, $CDCl_3$) δ = 184.05, 165.22, 149.63, 138.29, 133.47, 132.76, 129.74, 129.34, 128.77, 128.29, 126.66, 124.90, 122.95, 119.70, 119.63, 116.96, 113.31, 112.28, 59.86, 55.18, 22.89, 14.54. HRMS (ESI) Calcd. for $C_{23}H_{23}N_2O_2$ $[M+H]^+$: 359.1754, found 359.1744.

NB-4: Orange yellow solid, 143 mg, yield: 39 %. ^{1}H NMR (400 MHz, $CDCl_3$) δ 15.27 (s, 1H), 8.05 (d, *J* = 8.4 Hz, 1H), 7.97 (d, *J* = 8.1 Hz, 1H), 7.89 (dd, *J* = 26.7, 8.5 Hz, 2H), 7.72 (dd, *J* = 2.8, 1.3 Hz, 1H), 7.58 (ddd, *J* = 8.3, 6.9, 1.2 Hz, 1H), 7.51 – 7.45 (m, 1H), 6.98 (t, *J* = 1.6 Hz, 1H), 6.87 (d, *J* = 12.7 Hz, 1H), 6.14 (d, *J* = 12.7 Hz, 1H), 4.33 (q, *J* = 7.1 Hz, 2H), 1.63 (s, 6H), 1.38 (t, *J* = 7.1 Hz, 3H). ^{13}C NMR (101 MHz, $CDCl_3$) δ = 184.22, 164.78, 149.73, 137.92, 132.59, 131.81, 129.69, 129.53, 129.27, 128.69, 126.56, 125.67, 124.72, 122.80, 119.57, 118.08, 116.95, 109.89, 59.81, 55.02, 22.88, 14.47. HRMS (ESI) Calcd. for $C_{23}H_{23}N_2O_2$ $[M+H]^+$: 359.1754, found 359.1752.

3 Compared NMR data and spectra

Table S1 Experimental ^{1}H NMR chemical shifts of NB-1-4 for selective hydrogens in $CDCl_3$

Compounds	Chemical Shift/ppm (Coupling Constant *J*/Hz)		
	N…H-N	H1	H2
NB-1	15.90	8.02 (d, 13.0)	6.32 (d, 13.0)
NB-2	15.76	6.89 (d, 12.6)	6.12 (d, 12.6)
NB-3	15.49	8.02 (d, 13.1)	6.33 (d, 13.1)
NB-4	15.27	6.87 (d, 12.7)	6.14 (d, 12.7)

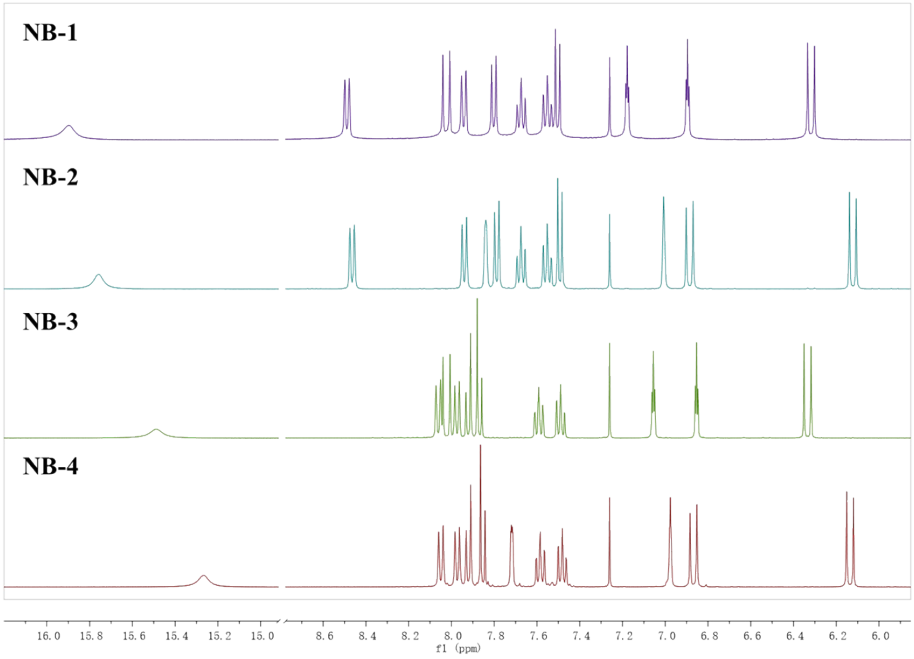

Figure S1. Comparison of partial ^{1}H NMR of NB-1-4 in $CDCl_3$

4 UV-Vis and fluorescence data

Table S2 Photophysical properties of **NB-1-4** in different solvents at room temperature.

Comp.	Solvent	Δf	λabs (ε/10^4 M-1 cm-1)(nm)	λex (nm)	λ_{em} (nm)	□□Δv		Φf in Solvents (%)	Φf in Solid (%)
						(nm)	(cm^{-1})		
NB-1	Toluene	0.02	428(4.04)	420	496, 570	142	5821	1.4	6.56
	DCM	0.22	424(4.62)		507, 572	148	6100	0.9	
	MeOH	0.31	421(4.09)		487, 573	152	6300	0.4	
	DMSO	0.26	426(3.93)		510, 572	146	5990	0.9	
NB-2	Toluene	0.02	412(2.42)	410	511, 558	146	6351	2.3	13.8
	DCM	0.22	410(2.89)		501, 559	149	6500	2.4	
	MeOH	0.31	406 (2.60)		465, 557	151	6680	1.0	
	DMSO	0.26	412(2.84)		561	149	6450	3.3	
NB-3	Toluene	0.02	416(3.69)	410	558	142	6120	1.5	23.0
	DCM	0.22	414 (5.22)		492, 561	147	6330	2.8	
	MeOH	0.31	410(4.62)		477, 557	147	6440	0.9	
	DMSO	0.26	415(4.38)		563	148	6330	2.5	
NB-4	Toluene	0.02	400(4.06)	400	546	146	6680	4.5	5.96
	DCM	0.22	402 (3.57)		485, 545	143	6530	3.7	
	MeOH	0.31	397(4.22)		543	164	7240	2.2	
	DMSO	0.26	400(4.5)		486, 548	148	6750	5.2	

Footnote: Fluorescence quantum yields were calculated using Rhodamine B (Φ_f = 0.49 in ethanol) or fluorescein (Φ_f = 0.90 in 0.1 N NaOH aqueous solution) as the reference.

Table S3 Photophysical properties of **NBs** in aggregates and solid at room temperature.

Comp.	Emission Enhancement Times in 95% H_2O:CH_3CN vs pure CH_3CN (λ_{em} (nm))	Emission Enhancement Times in 95% H_2O:DMSO vs pure DMSO (λ_{em} (nm))	Emission Enhancement Times in 95% H_2O:DMF vs pure DMF (λ_{em} (nm))	Emission Enhancement Times in solid vs pure Toluene (λ_{em} (nm))
NB-1	7.1 (586)	3.3 (586)	2.8 (586)	4.7 (594, 629)
NB-2	9.2 (572)	4.1 (572)	5.0 (571)	6.0 (575, 615)
NB-3	8.4 (570)	3.7 (572)[a]	8.0 (564)	15.3 (593, 631)
NB-4	11.1 (555)	4.4 (555)[a]	4.5 (555)[a]	1.3 (556, 598)

Footnote: [a] Emission Enhancement in 90% H_2O:Solvents vs pure Solvents

Crystal data

Table S4 Crystal data and structure refinement for **NB-1,3**

Name	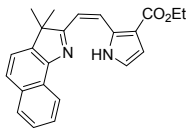 NB-1	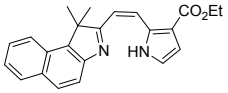 **NB-3**
Formula	$C_{23}H_{22}N_2O_2$	$C_{23}H_{22}N_2O_2$
Formula Weight	358.42	358.42
Crystal system	Monoclinic	Monoclinic
T (K)	113.15	113(2)
Space group	C2/c	P2(1)/n
a (Å)	21.762(4)	9.6810(19)
b (Å)	6.5576(13)	11.462(2)
c (Å)	27.605(6)	16.848(3)
α (deg)	90	90
β (deg)	100.00(3)	98.17(3)
γ (deg)	90	90
V (Å3)	3879.5(14)	1850.5(7)
Z	8	4
D_{calc} (g cm^{-3})	1.227	1.286
μ [mm^{-1}]	0.079	0.083
F (000)	1520.0	760

Crystal size (mm)	0.2 x 0.18 x 0.12	0.200 x 0.180 x 0.12(
$2\theta_{min}$, $2\theta_{max}$ (deg)	4.412, 55.802	2.156, 27.903
No. of reflns measd (unique)	4618	4389
No. of rflns measd (I > 2□(*I*))	21928	19376
parameters	252	250
Goodness-of-fit	1.098	1.012
R_1	0.0728	0.0996
wR_2 (all data)	0.1429	0.1181
Δ (□□Å^{-3})	0.27, -0.23	0.502, –0.303
CCDC number	1954587	1954588

5 UV-Vis and fluorescence spectra

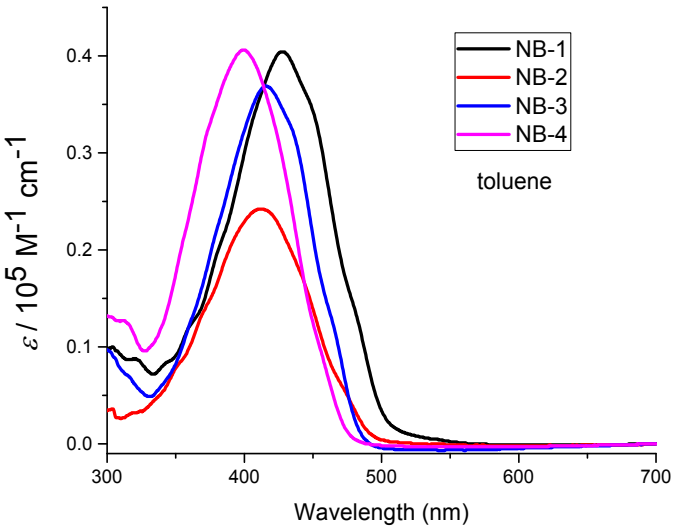

Figure S2 UV-Vis spectra of **NB-1-4** in toluene

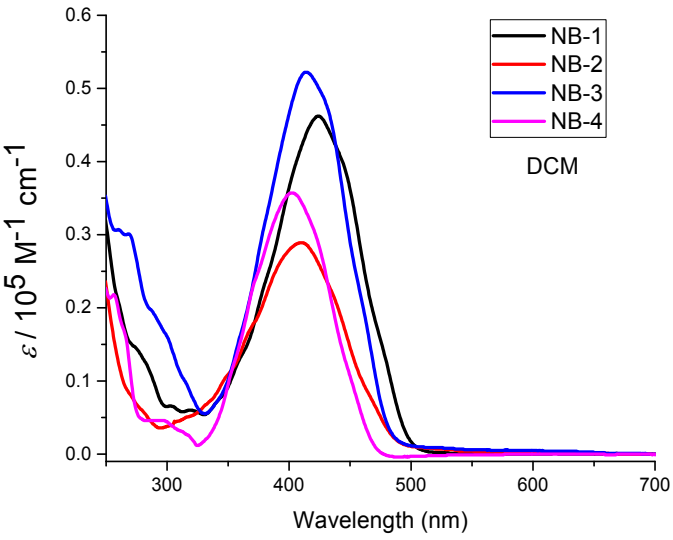

Figure S3 UV-Vis spectra of **NB-1-4** in DCM

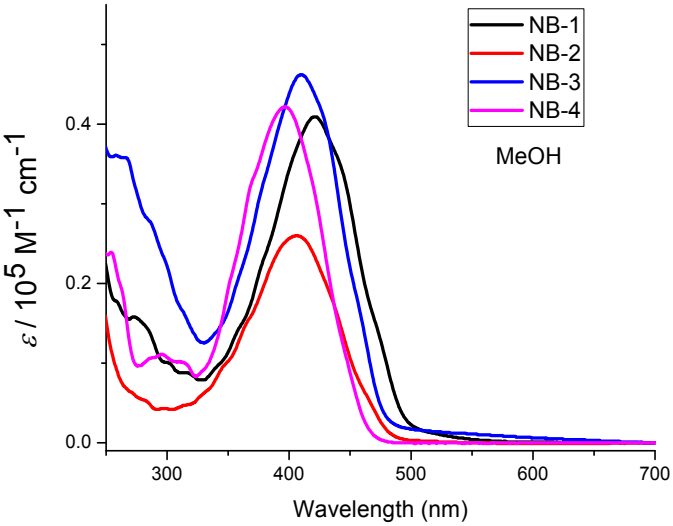

Figure S4 UV-Vis spectra of **NB-1-4** in MeOH

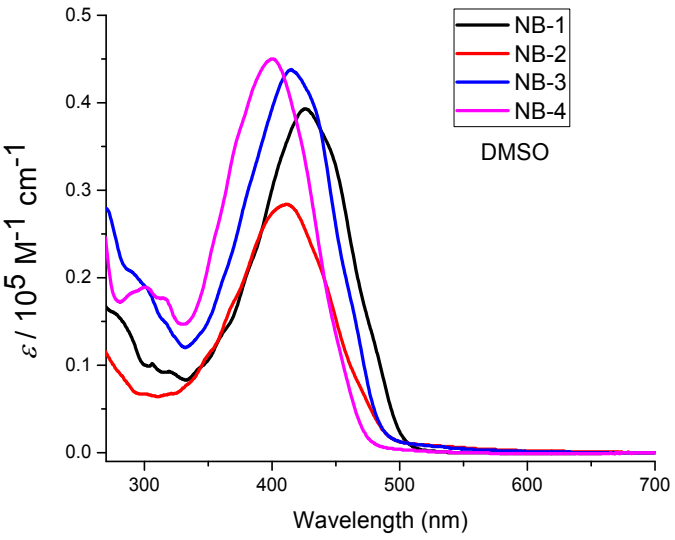

Figure S5 UV-Vis spectra of **NB-1-4** in DMSO

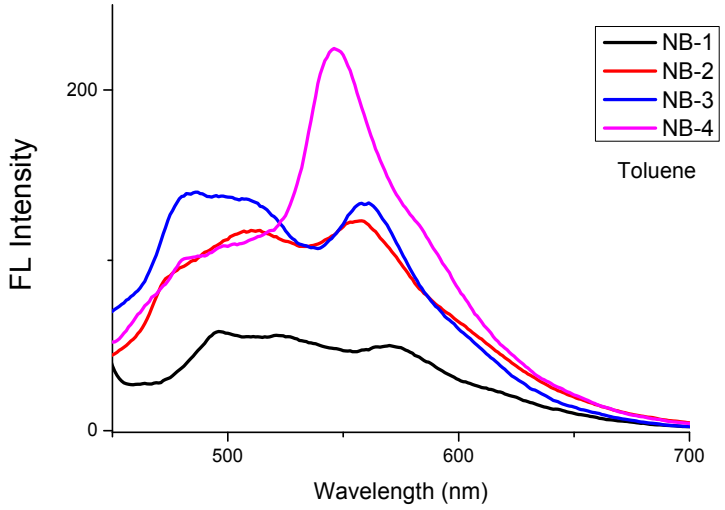

Figure S6 Fluorescence spectra of **NB-1-4** in toluene

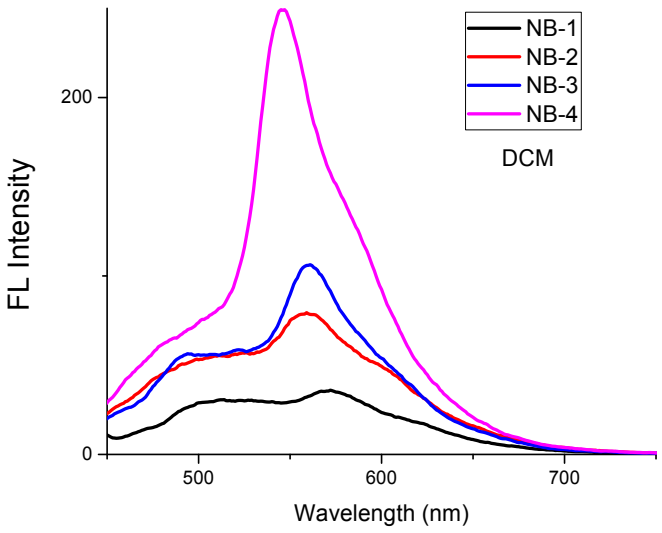

Figure S7 Fluorescence spectra of **NB-1-4** in DCM

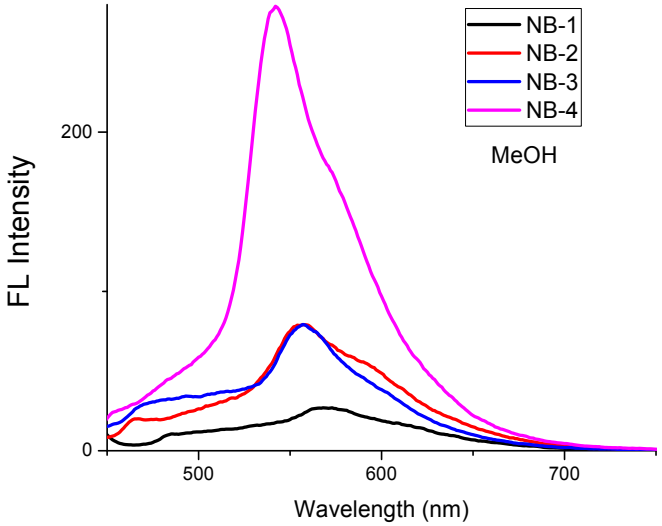

Figure S8 Fluorescence spectra of **NB-1-4** in MeOH

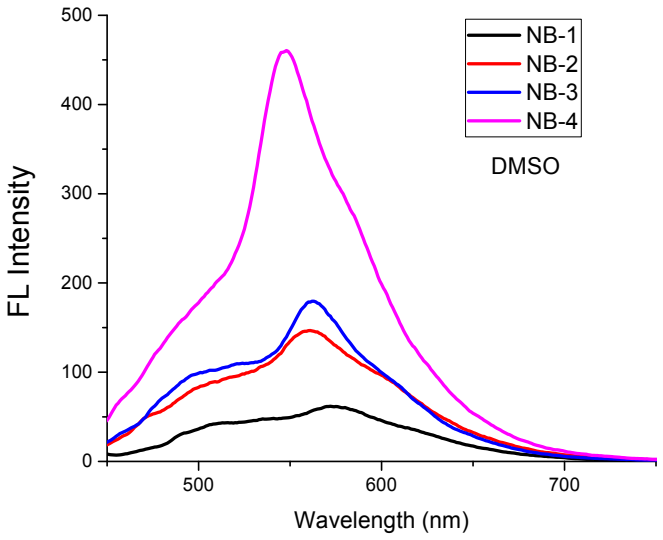

Figure S9 Fluorescence spectra of **NB-1-4** in DMSO

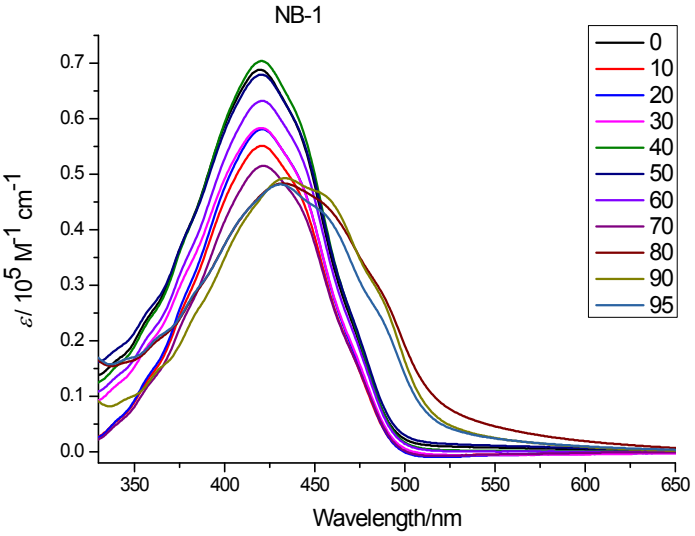

Figure S10 Absorption spectra of 10 μM NB-1 in the CH3CN/H2O mixture at different water fractions.

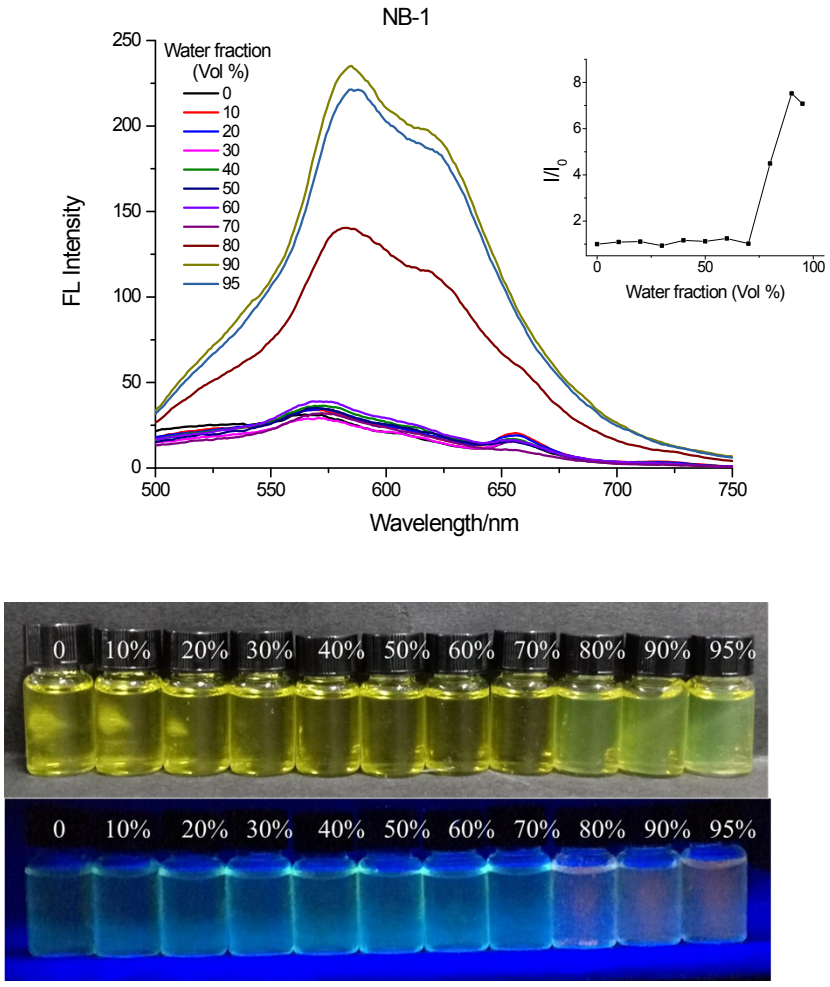

Figure S11 Fluorescence spectra and relative fluorescence intensity (I/I_0, inset) of 10 μM NB-1 in the CH3CN/H2O mixture at different water fractions excited at 365 nm.

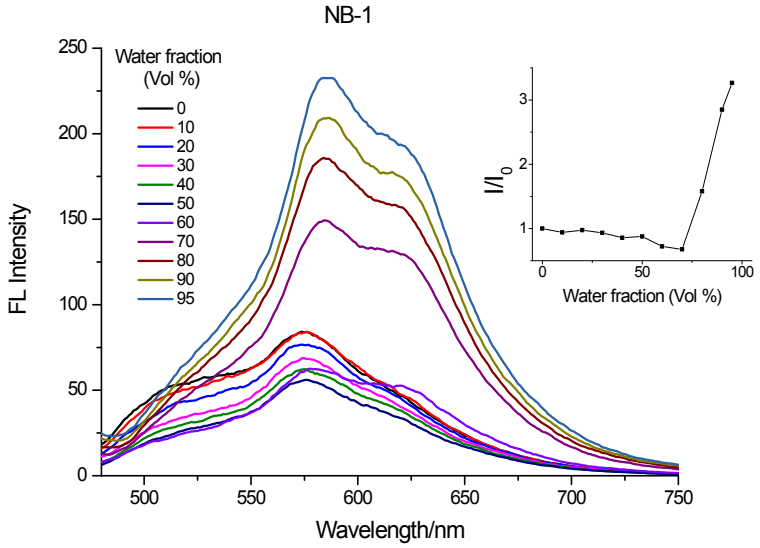

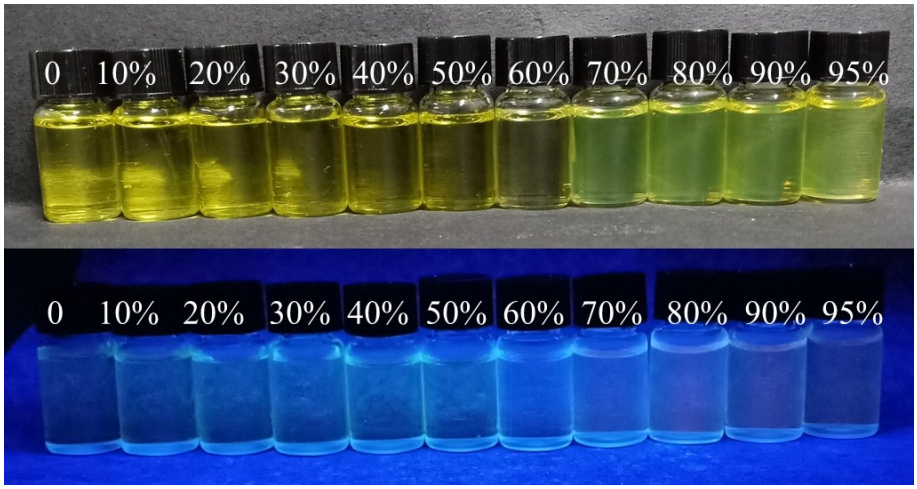

Figure S12 Fluorescence spectra and relative fluorescence intensity (I/I_0, inset) of 10 μM NB-1 in the DMSO/H2O mixture at different water fractions excited at 365 nm.

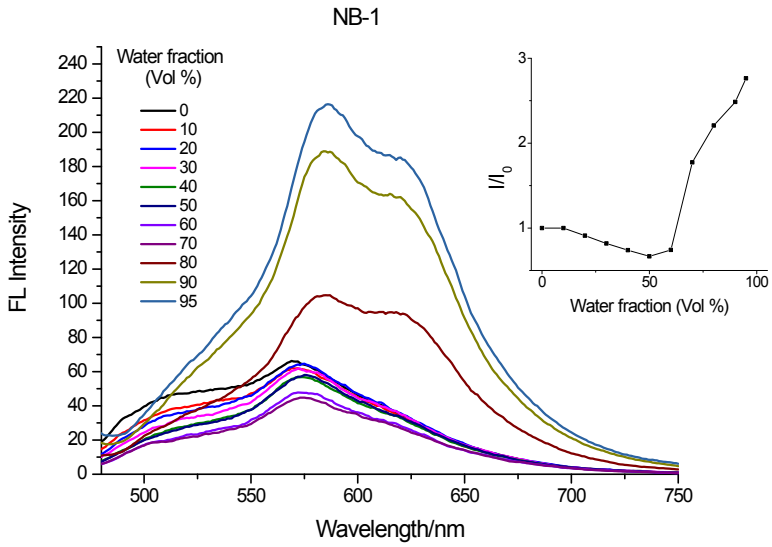

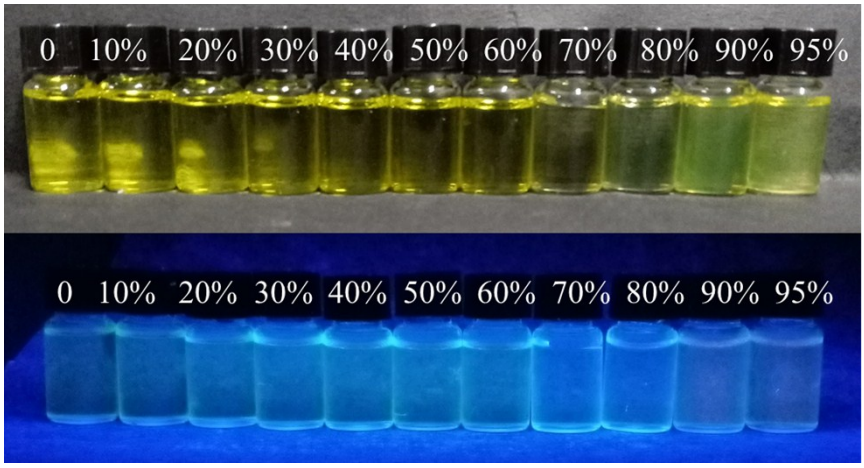

Figure S13 Fluorescence spectra and relative fluorescence intensity (I/I_0, inset) of 10 μM NB-1 in the DMF/H2O mixture at different water fractions excited at 365 nm.

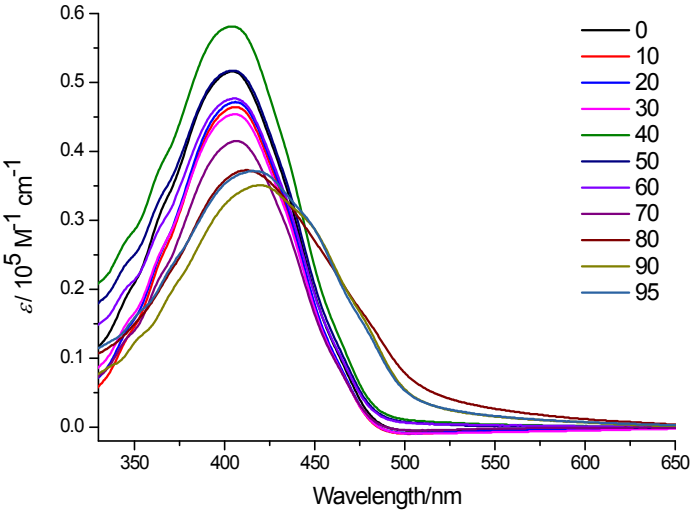

Figure S14 Absorption spectra of 10 □M NB-2 in the CH3CN/H2O mixture at different water fractions.

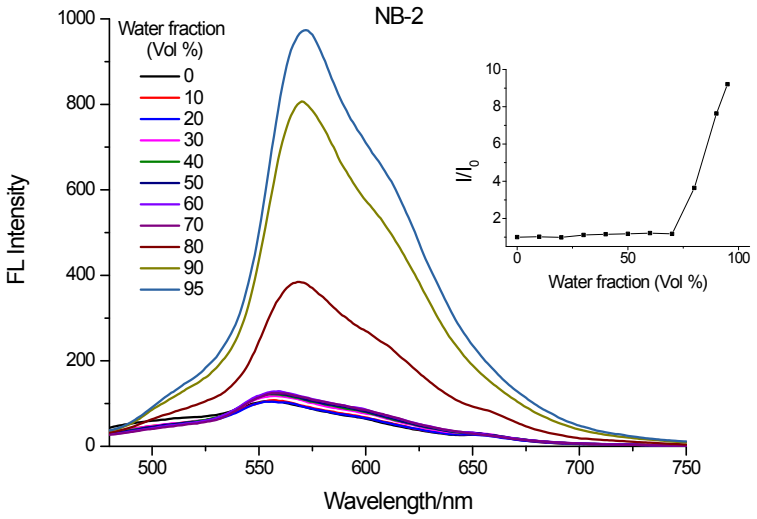

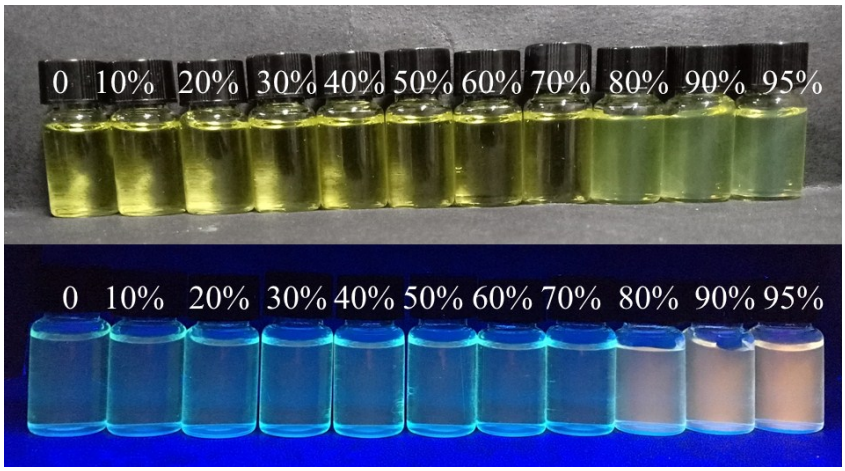

Figure S15 Fluorescence spectra and relative fluorescence intensity (I/I_0, inset) of 10 μM NB-2 in the CH3CN/H2O mixture at different water fractions excited at 365 nm.

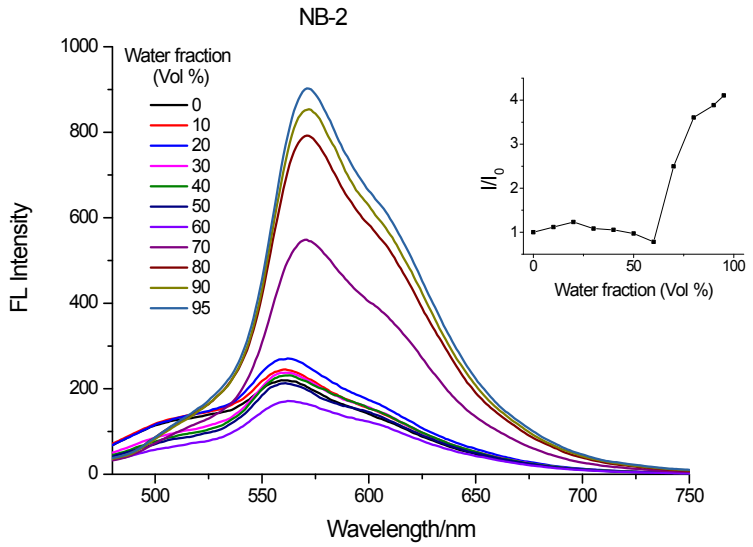

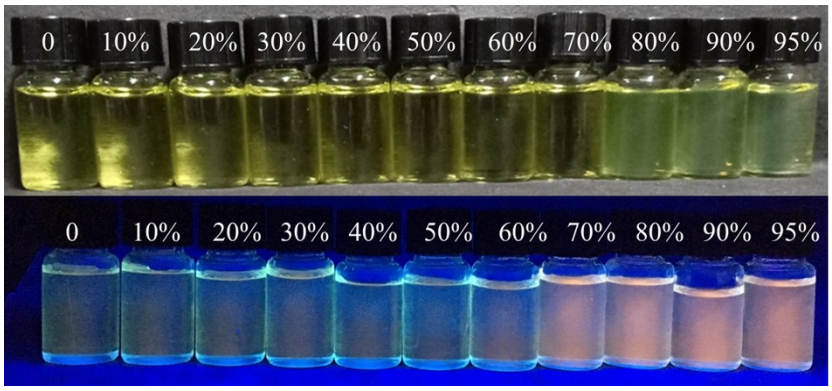

Figure S16 Fluorescence spectra and relative fluorescence intensity (I/I_0, inset) of 10 μM NB-2 in the DMSO/H2O mixture at different water fractions excited at 365 nm.

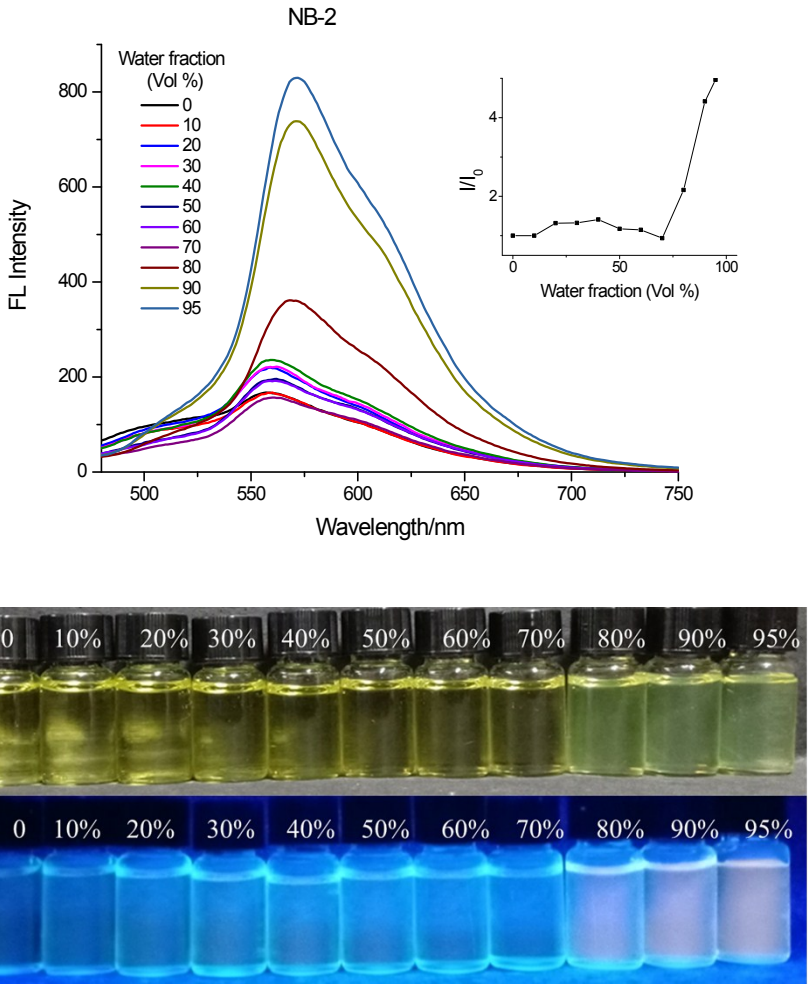

Figure S17 Fluorescence spectra and relative fluorescence intensity (I/I_0, inset) of 10 μM NB-2 in the DMF/H2O mixture at different water fractions excited at 365 nm.

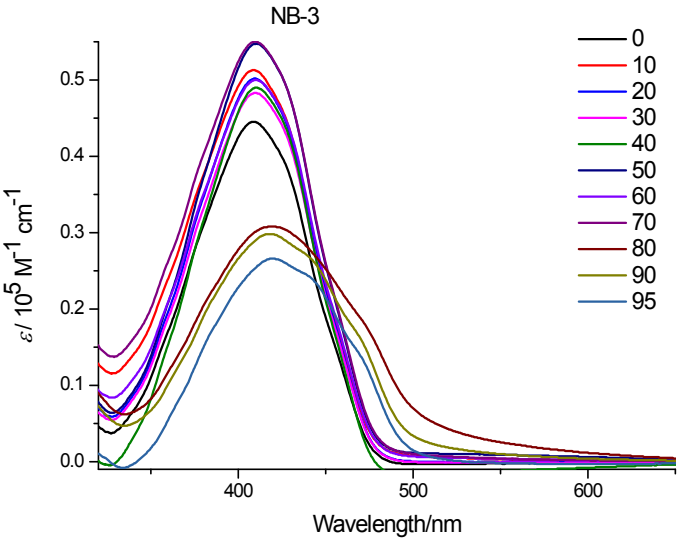

Figure S18 Absorption spectra of 10 □M NB-3 in the CH3CN/H2O mixture at different water fractions.

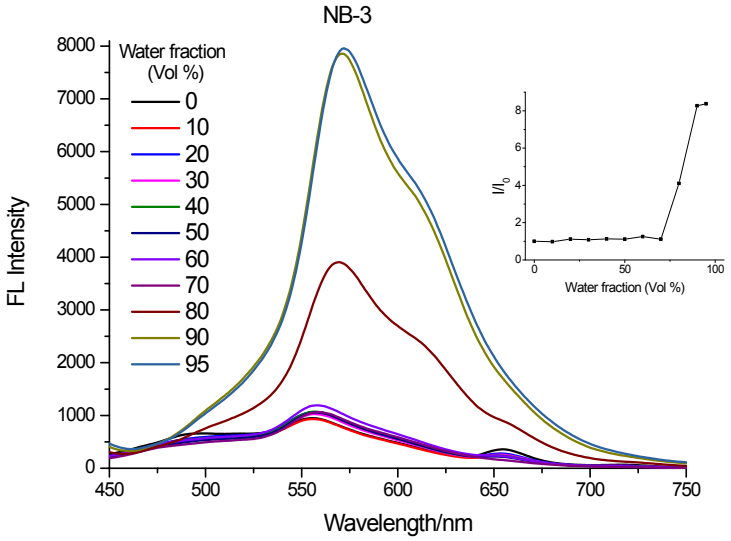

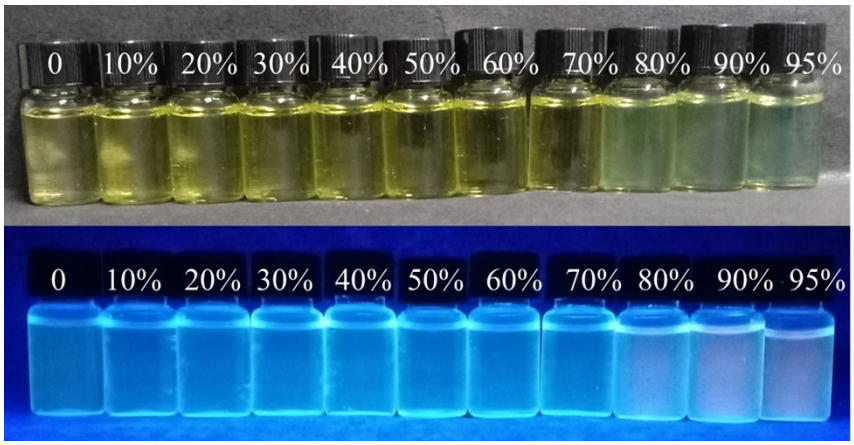

Figure S19 Fluorescence spectra and relative fluorescence intensity (I/I_0, inset) of 10 μM NB-3 in the CH3CN/H2O mixture at different water fractions excited at 365 nm.

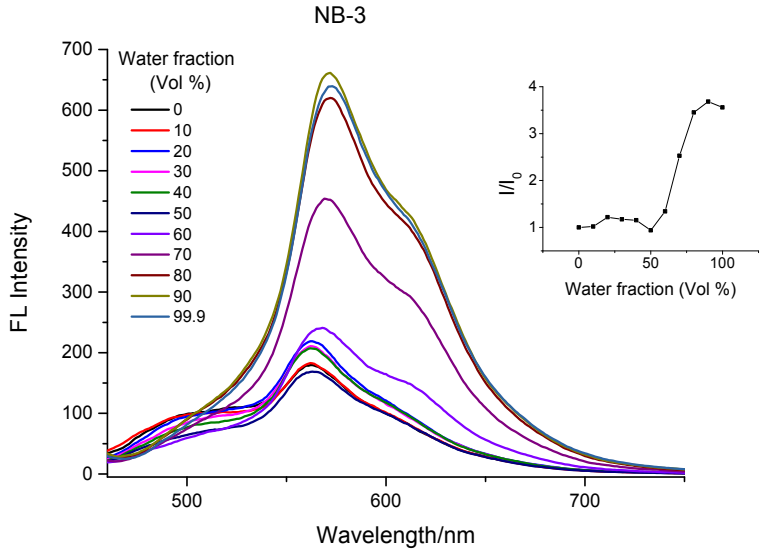

Figure S20 Fluorescence spectra and relative fluorescence intensity (I/I_0, inset) of 10 μM NB-3 in the DMSO/H2O mixture at different water fractions excited at 365 nm.

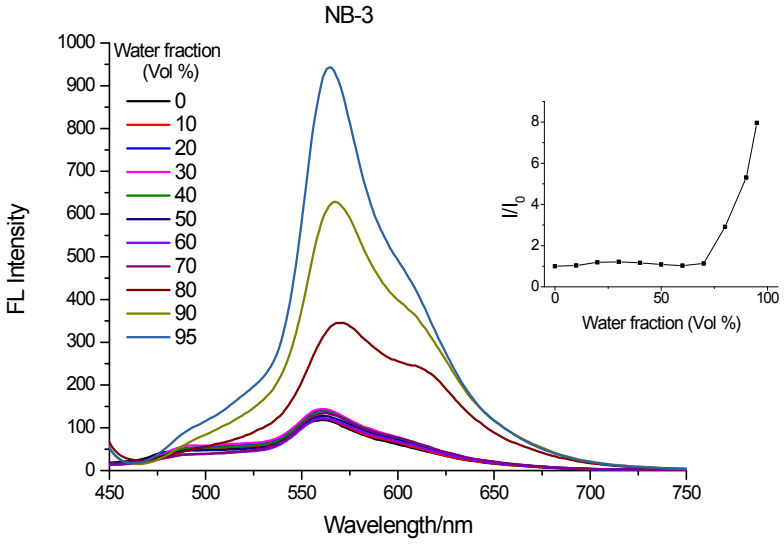

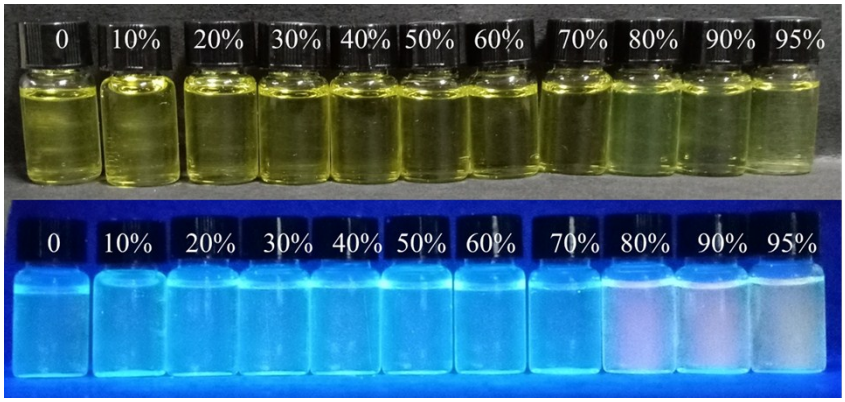

Figure S21 Fluorescence spectra and relative fluorescence intensity (I/I_0, inset) of 10 μM NB-3 in the DMF/H2O mixture at different water fractions excited at 365 nm.

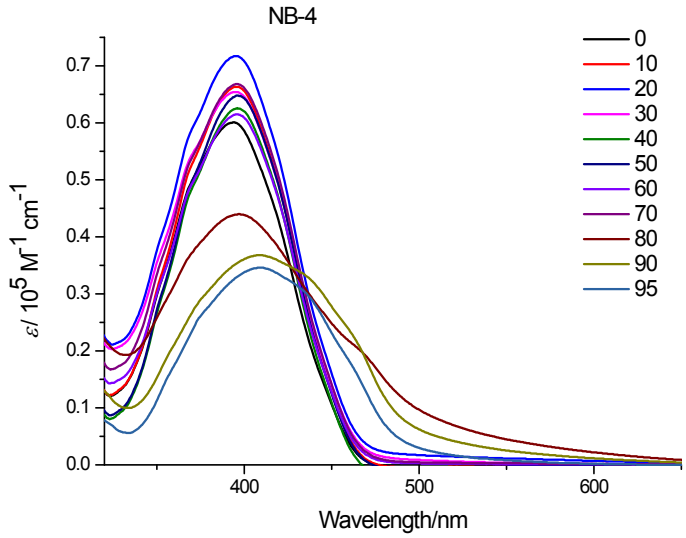

Figure S22 Absorption spectra of 10 □M NB-4 in the CH3CN/H2O mixture at different water fractions.

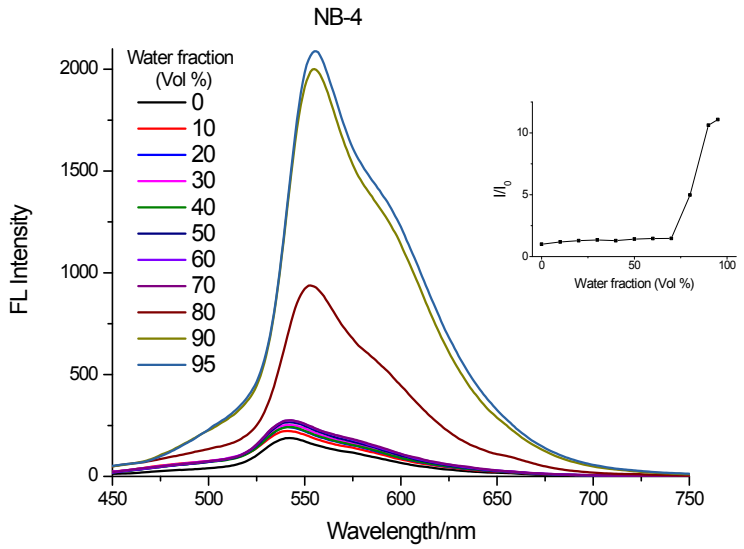

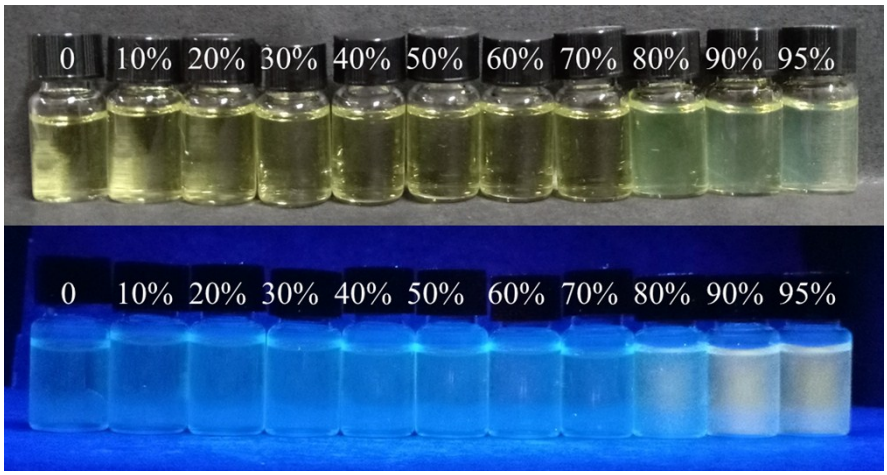

Figure S23 Fluorescence spectra and relative fluorescence intensity (I/I_0, inset) of 10 μM NB-4 in the CH3CN/H2O mixture at different water fractions excited at 365 nm.

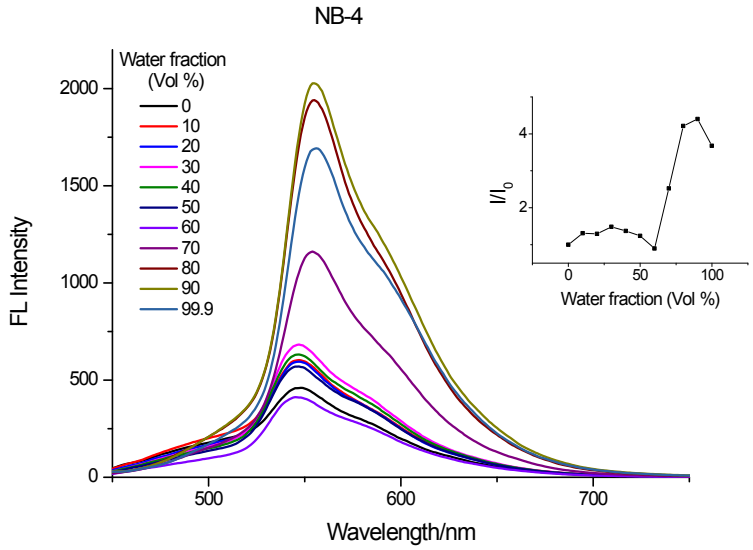

Figure S24 Fluorescence spectra and relative fluorescence intensity (I/I_0, inset) of 10 μM NB-4 in the DMSO/H2O mixture at different water fractions excited at 365 nm.

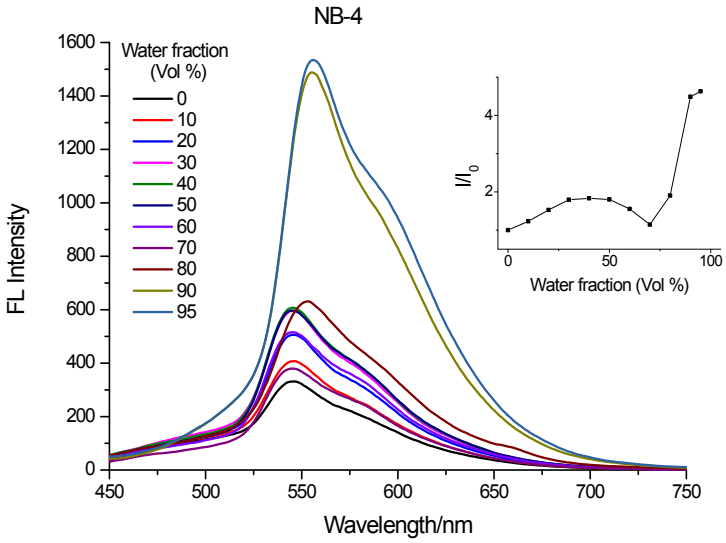

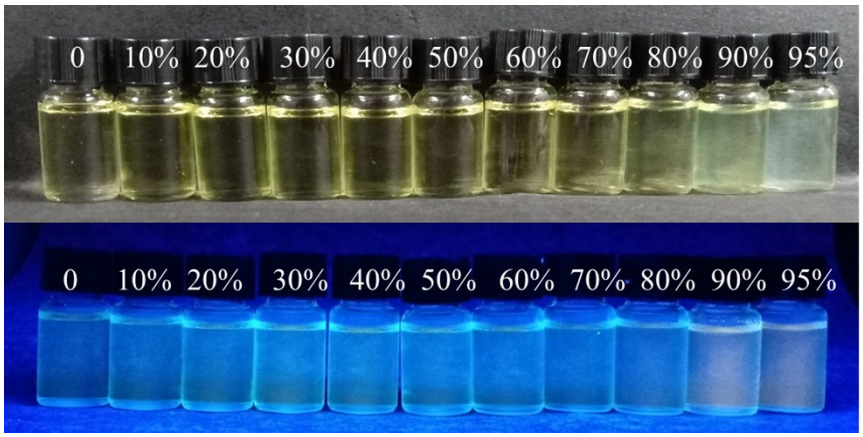

Figure S25 Fluorescence spectra and relative fluorescence intensity (I/I_0, inset) of 10 μM NB-4 in the DMF/H2O mixture at different water fractions excited at 365 nm.

6 Optimal and crystal structure

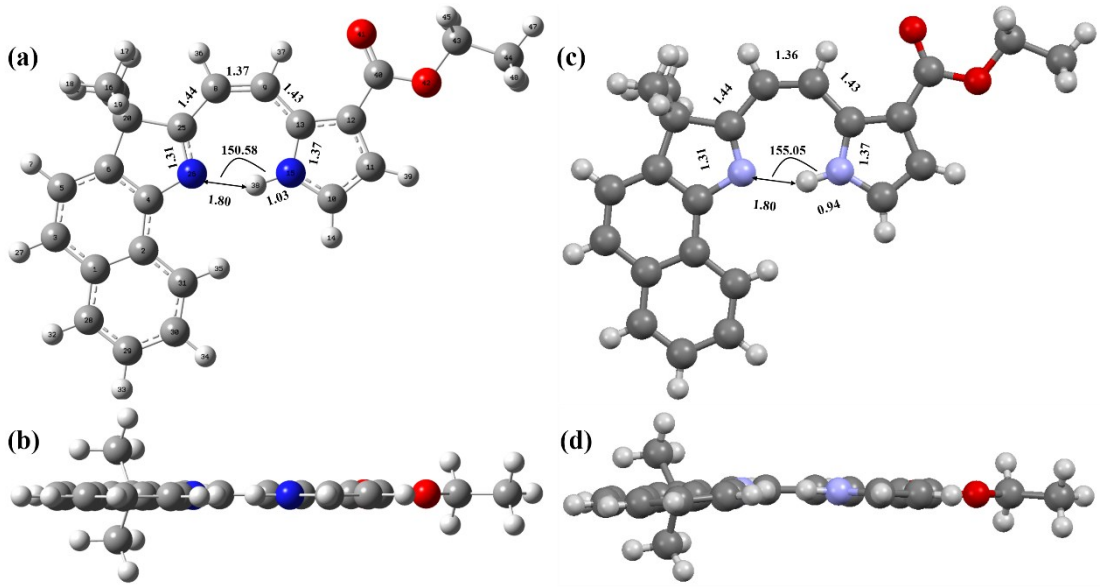

Figure S26 Comparing of optimal structure by calculation and crystal structure of typical bond lengths and angle for **NB-1**. **(a)** optimal structure by calculation, top view; **(a)** optimal structure by calculation, side view; **(c)** crystal structure, top view; **(d)** crystal structure, side view.

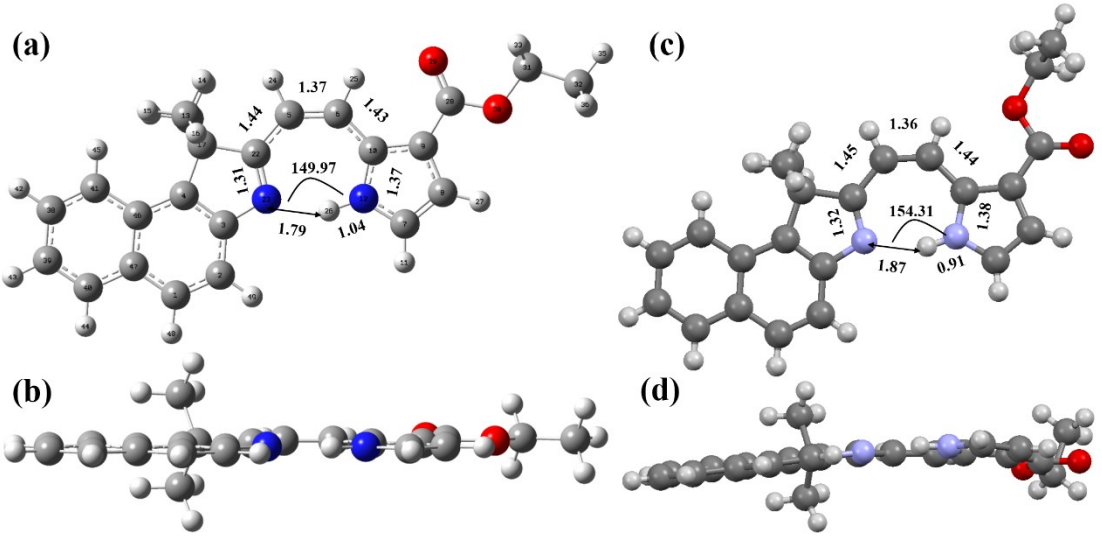

Figure S27 Comparing of optimal structure by calculation and crystal structure of typical bond lengths and angle for **NB-3**. **(a)** optimal structure by calculation, top view; **(a)** optimal structure by calculation, side view; **(c)** crystal structure, top view; **(d)** crystal structure, side view.

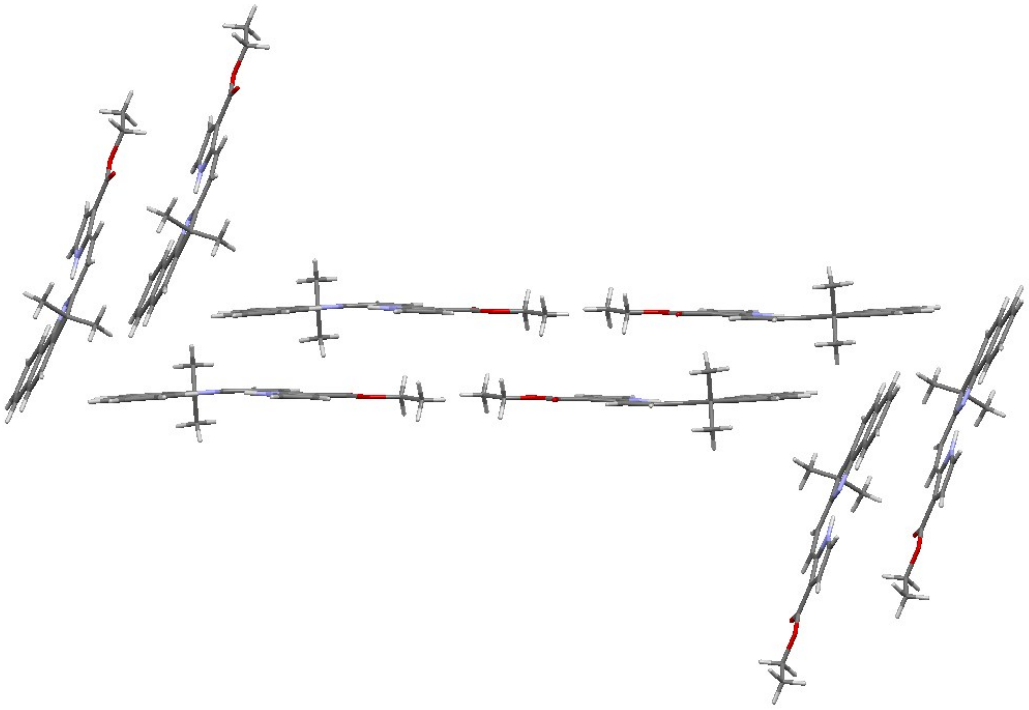

Figure S28 Crystal packing sideview of NB-1

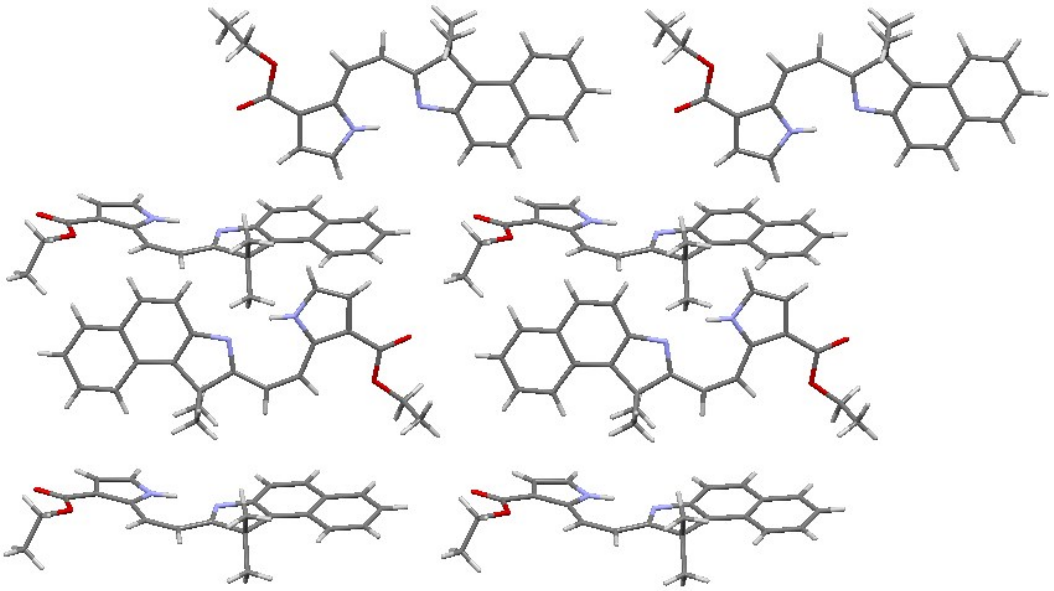

Figure S29 Crystal packing sideview of NB-3

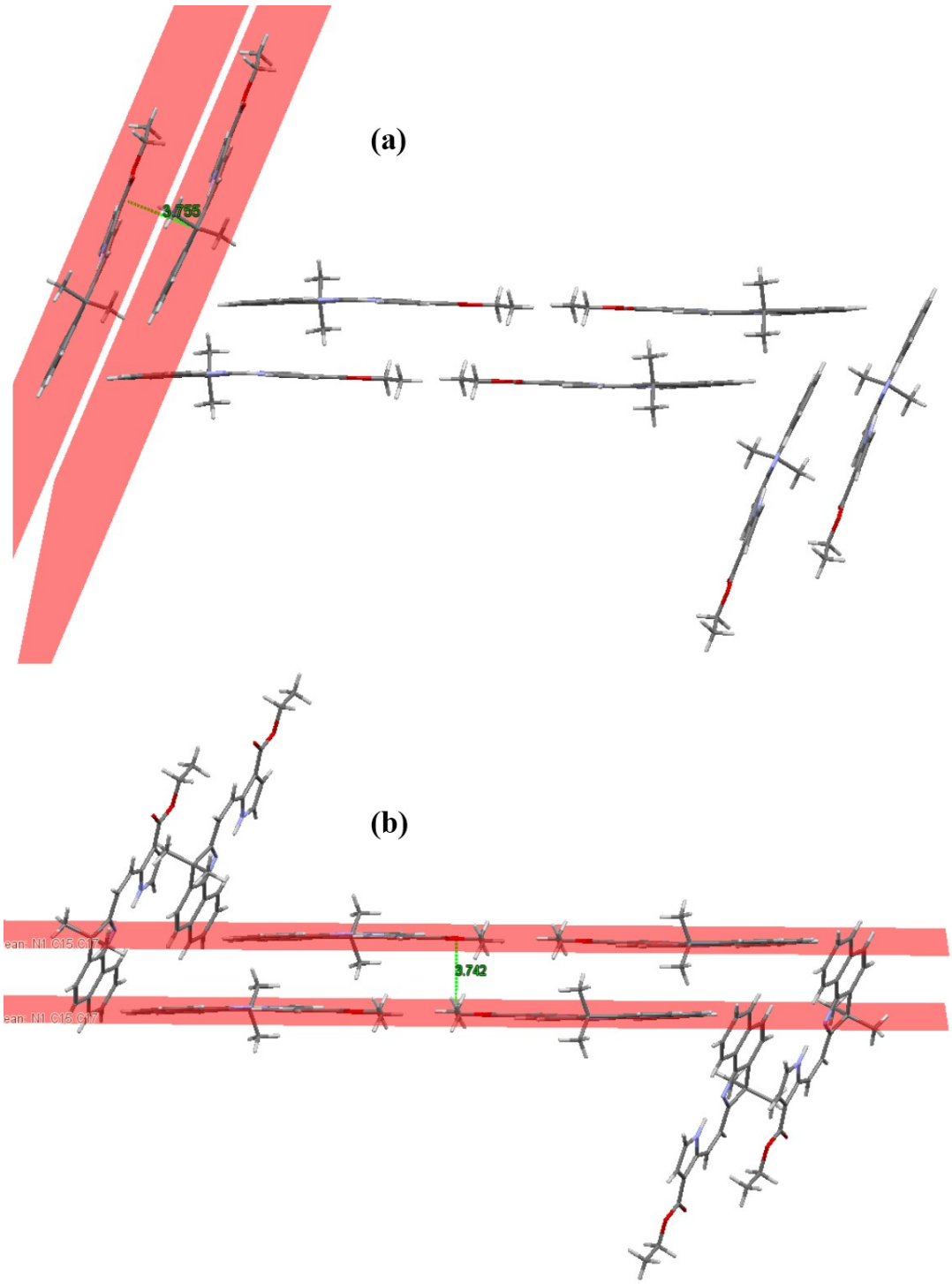

Figure S30 The distance of planes of NB-1

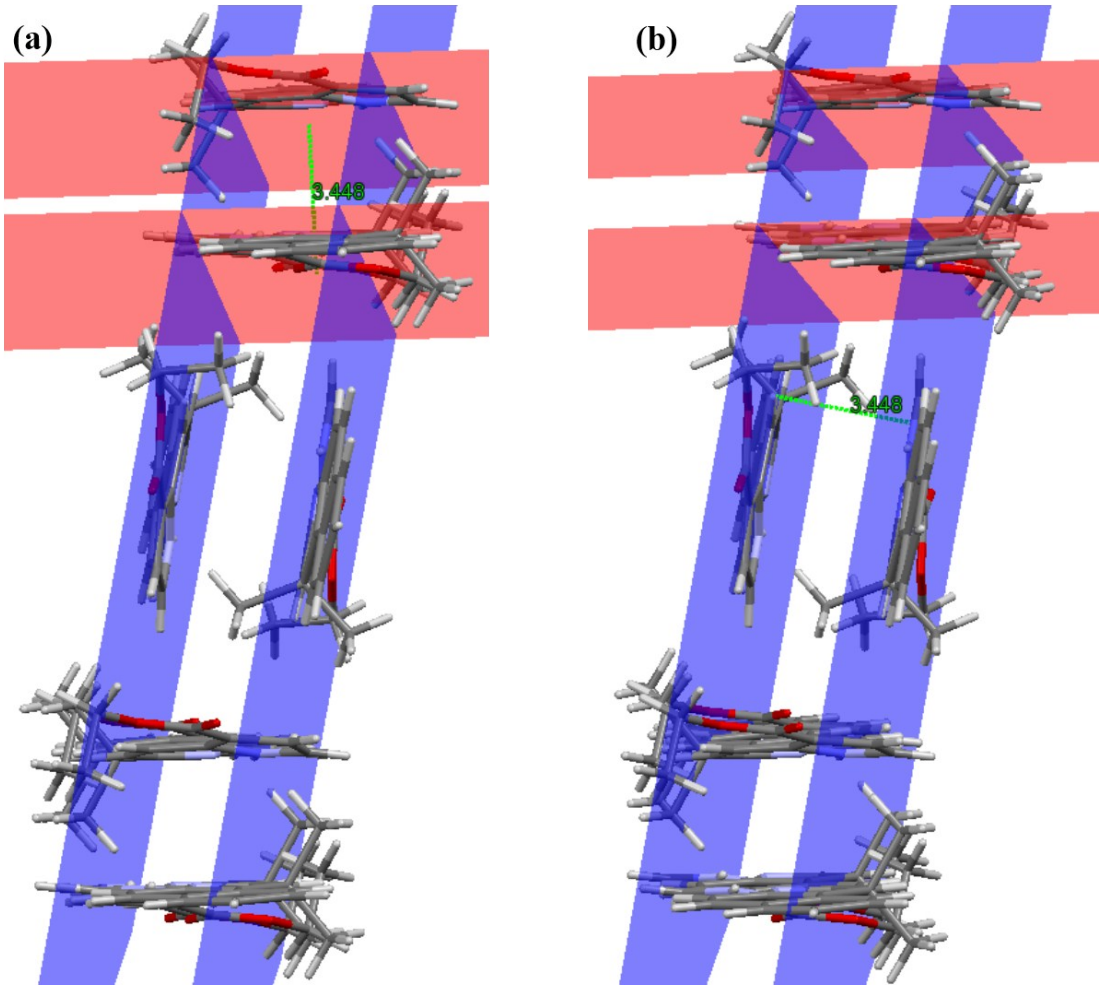

Figure S31 The distance of planes of NB-3

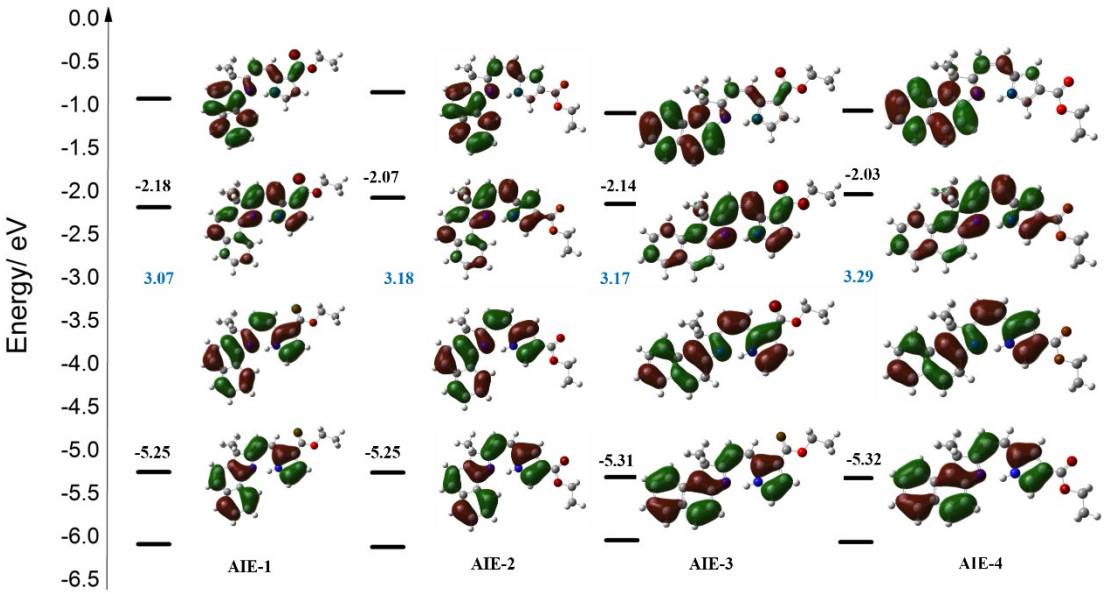

Figure S32 Electron distribution, energy for selected four frontier orbital and energy gap (blue) of **NB-1-4** at level B3LYP/6-311G(d)

7 Calculated data and tables

Table S5 The major transition configuration of excited states of **NB-1-4** in toluene

name	Wavelength (nm)	Osc. Strength	Major contribs (>15%)
NB-1	459.86	0.7529	HOMO->LUMO (99.8%)
	359.74	0.0938	H-1->LUMO (89.4%)
NB-2	426.48	0.5905	HOMO->LUMO (99.2%)
	346.34	0.0833	H-1->LUMO (81.6%), HOMO->L+1 (15.8%)
NB-3	443.49	0.9495	HOMO->LUMO (99.7%)
	366.07	0.0554	H-1->LUMO (85.7%), HOMO->L+1 (10.8%)
	329.01	0.0520	HOMO->L+1 (77.7%), H-1->LUMO (12.3%)
	315.24	0.0870	H-2->LUMO (82.0%)
	295.27	0.0535	H-3->LUMO (96.1%)
	267.82	0.1300	H-1-> L+1 (39.5%), HOMO->L+2 (29.8%), H-2-> L+1 (14.9%)
NB-4	426.57	0.9462	HOMO->LUMO (99.5%)
	355.94	0.0533	H-1->LUMO (78.4%), HOMO->L+1 (17.4%)
	325.26	0.1020	HOMO->L+1 (72.5%), H-1->LUMO (19.2%)
	305.69	0.0949	H-2->LUMO (83.7%)
	274.68	0.0555	H-1-> L+1 (68.0%), HOMO->L+3 (24.1%)
	260.70	0.1237	H-2-> L+1 (37.4%), HOMO->L+3 (22.4%), H-1-> L+1 (16.8%)

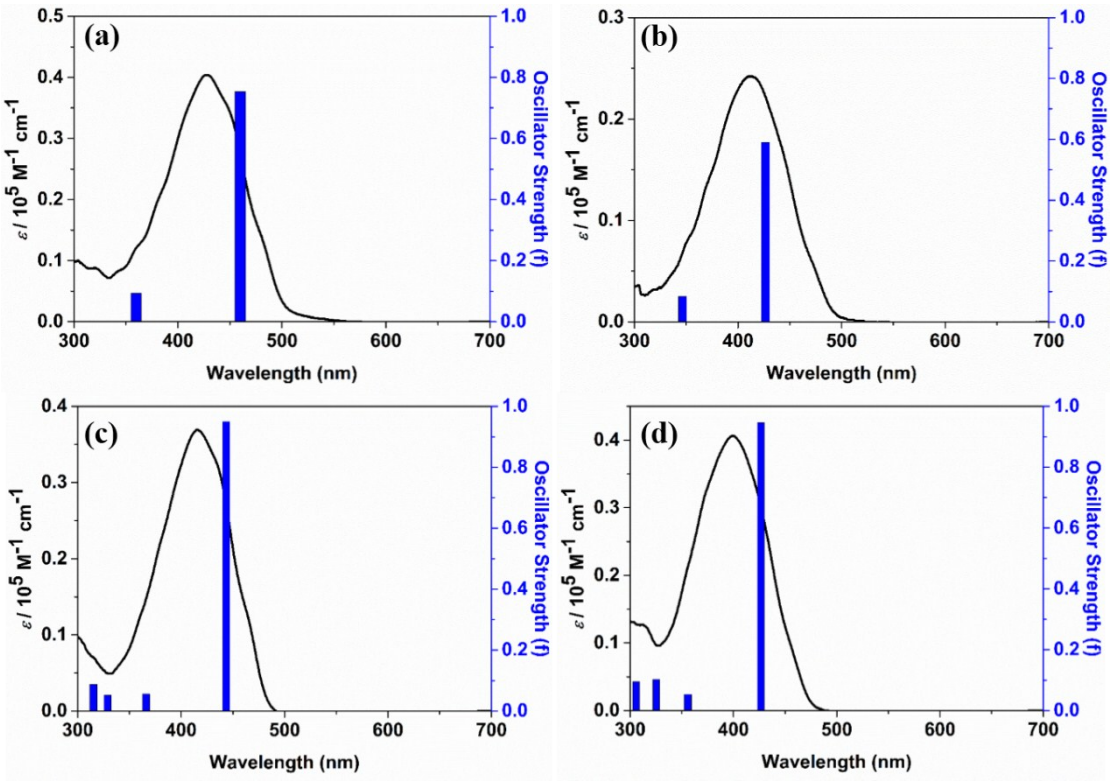

Figure S33 TD-DFT (B3LYP/6-31G(d)) simulated stick spectra (blue columnar) along with their normalized steady-state absorption spectra (black solid lines)

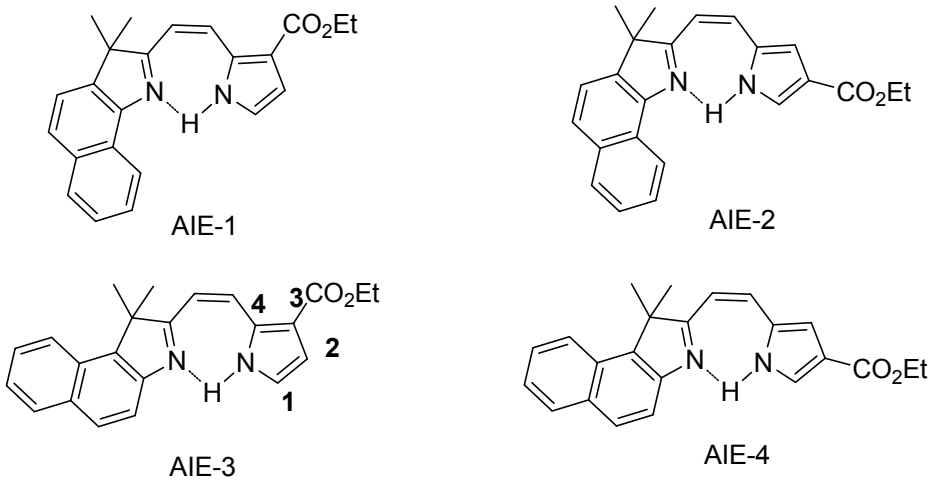

Table S6 Bond distance and angle of **NB**s in toluene in N-S_0, N-S_1, T-S_1 states based on DFT and TDDFT calculations

Entry	Category	N-S_0	N-S_1	Change between N-S_1 and N-S_0	T-S_1
NB-1	N-H(Å)	1.03477	1.03774	0.00297	1.67157
	N...H(Å)	1.79950	1.79402	0.00548	1.06268
	Angle(º)	150.58291	151.70712	1.12421	155.33556
NB-2	N-H(Å)	1.03430	1.04080	0.0065	1.67937
	N...H(Å)	1.81512	1.78167	0.03345	1.06036

	Angle(º)	149.06926	151.39336	2.3241	155.59140
NB-3	N-H(Å)	1.03521	1.03910	0.00389	1.67451
	N...H(Å)	1.79356	1.78625	0.00731	1.06382
	Angle(º)	149.97125	151.10205	1.1308	154.32537
NB-4	N-H(Å)	1.03471	1.04217	0.00746	1.68083
	N...H(Å)	1.80956	1.77440	0.03516	1.06237
	Angle(º)	148.39566	150.78303	2.38737	154.54615

Table S7 Calculated potential energy of **NBs** in toluene in N-S_1, highest energy in S_1 state (H-S_1), T-S_1 states based on DFT and TDDFT calculations

Entry	Energy (hartree)			ΔE_1 (Kcal/ mol)	ΔE_2 (Kcal/ mol)
	N-S_1	H-S_1	T-S_1		
NB-1	-1149.59935	-1149.58866	-1149.59148	4.935	6.708
NB-2	-1149.59601	-1149.58690	-1149.59033	3.564	5.717
NB-3	-1149.59325	-1149.58285	-1149.58546	4.888	6.526
NB-4	-1149.58979	-1149.58094	-1149.58406	3.596	5.553

Note: $\Delta E\,(eV) = E_{T\text{-}S1}\text{-}E_{N\text{-}S1}$; $\Delta E\,(eV) = E_{H\text{-}S1}\text{-}E_{N\text{-}S1}$

8 ^{1}H, ^{13}C-NMR and HRMS spectra

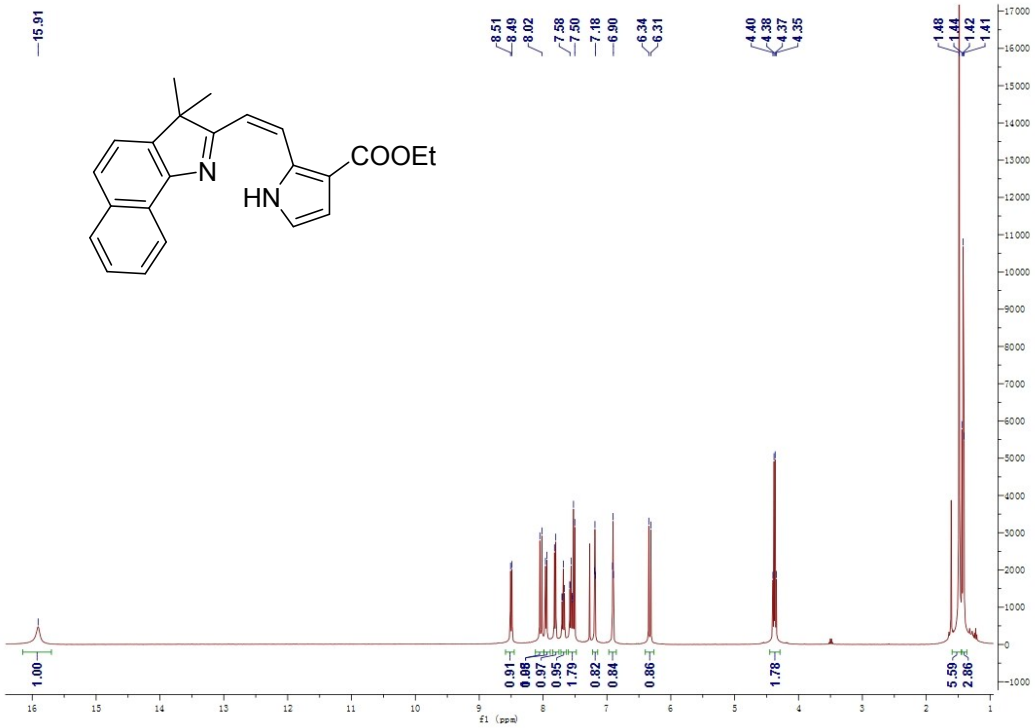

Figure S34 ^{1}H NMR spectra of **NB-1**

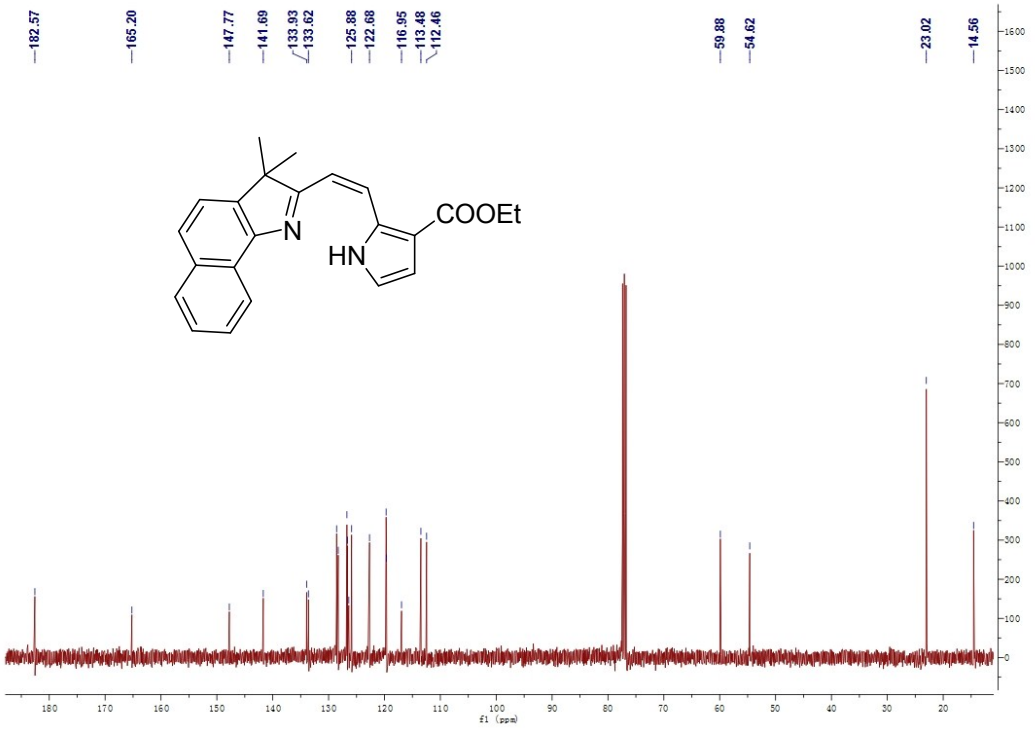

Figure S35 ^{13}C NMR spectra of **NB-1**

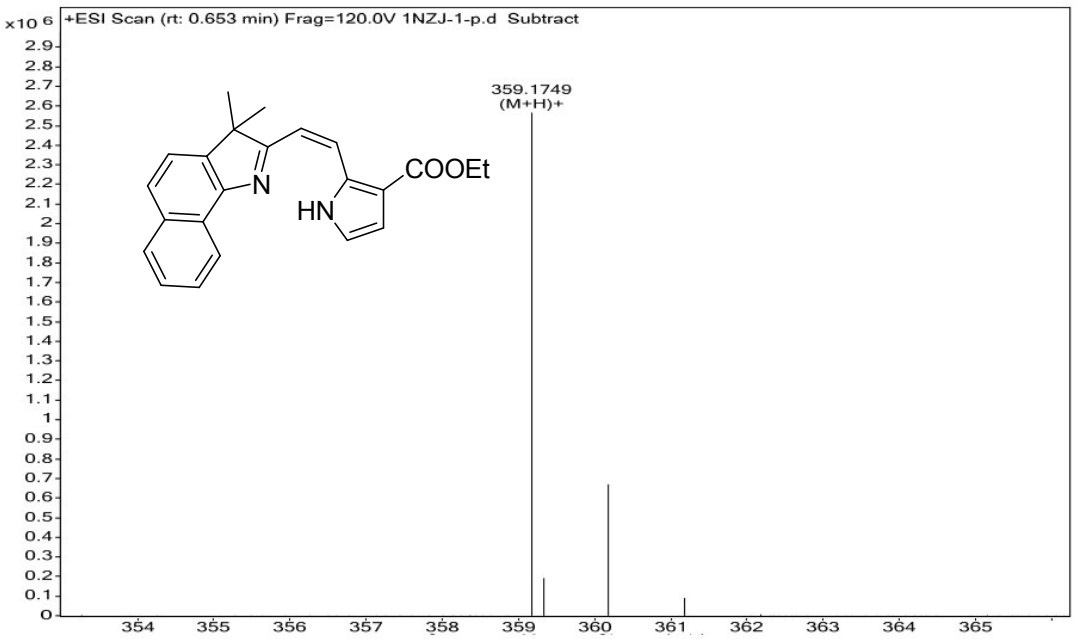

Figure S36 HRMS (ESI) spectra of **NB-1**

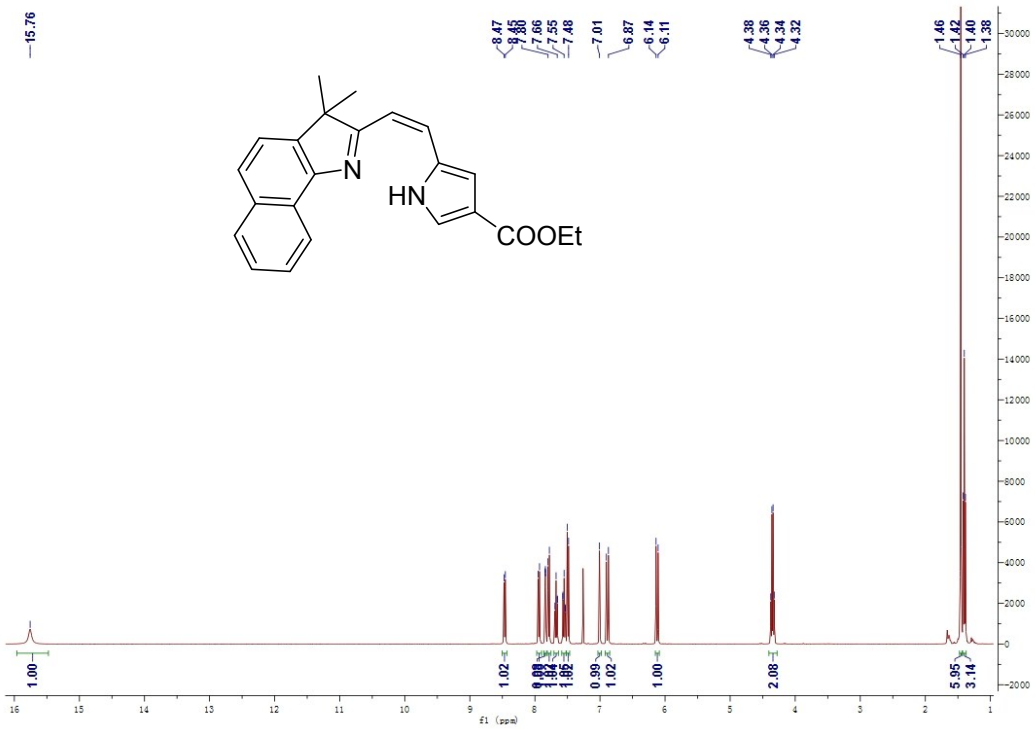

Figure S37 ^{1}H NMR spectra of **NB-2**

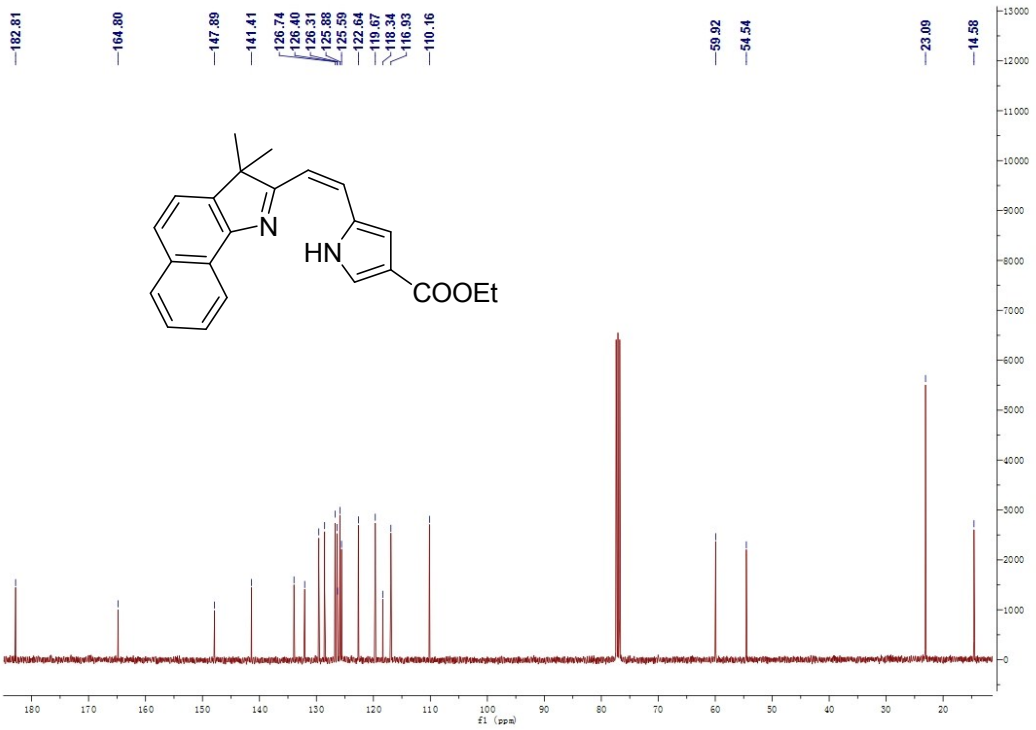

Figure S38 ^{13}C NMR spectra of **NB-2**

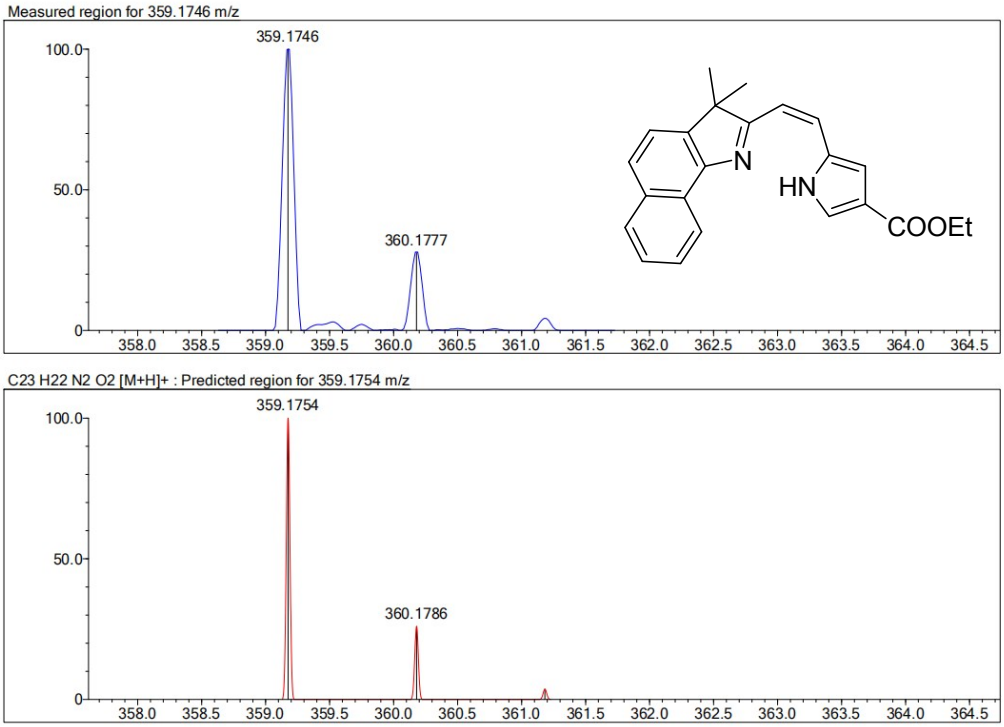

Figure S39 HRMS (ESI) spectra of **NB-2**

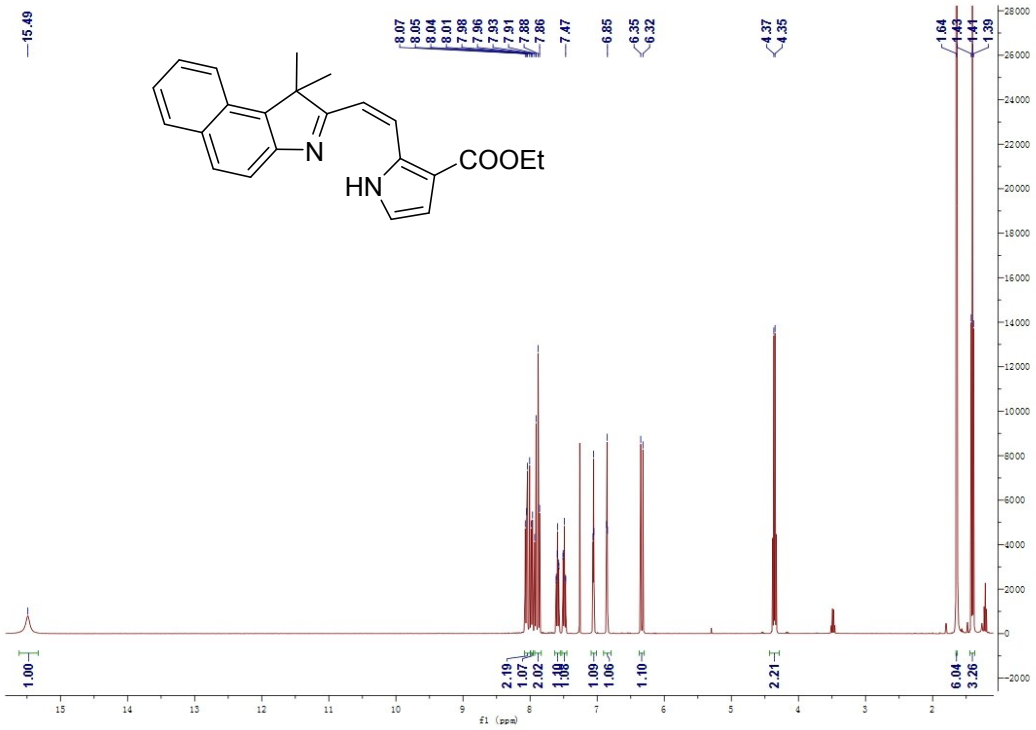

Figure S40 ^{1}H NMR spectra of **NB-3**

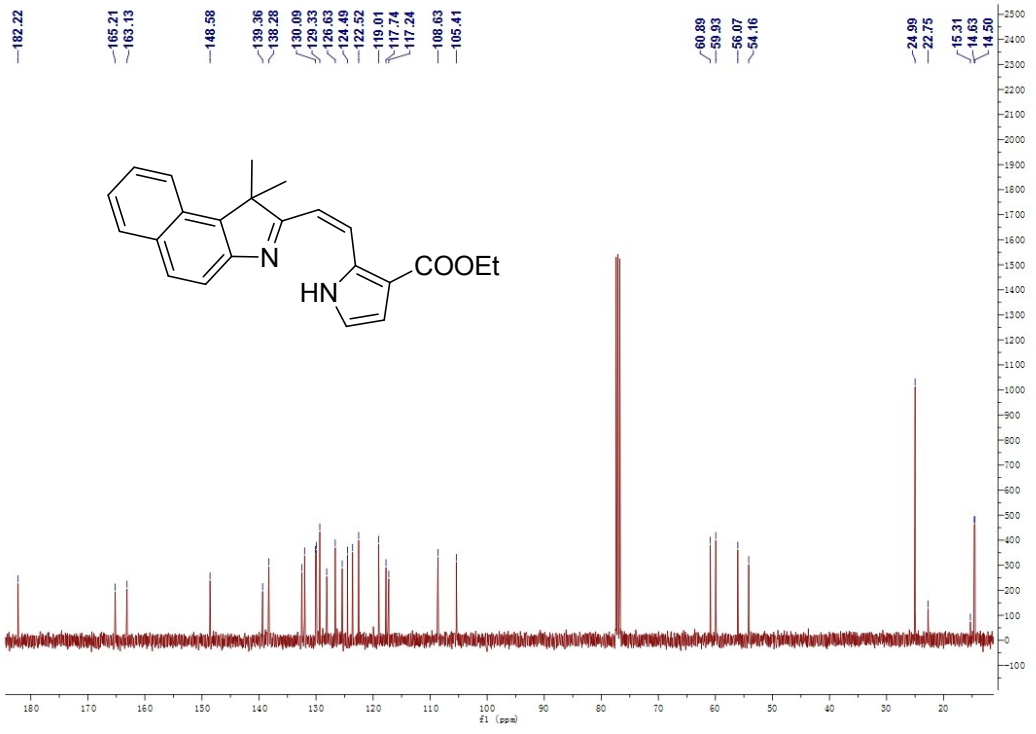

Figure S41 ^{13}C NMR spectra of **NB-3**

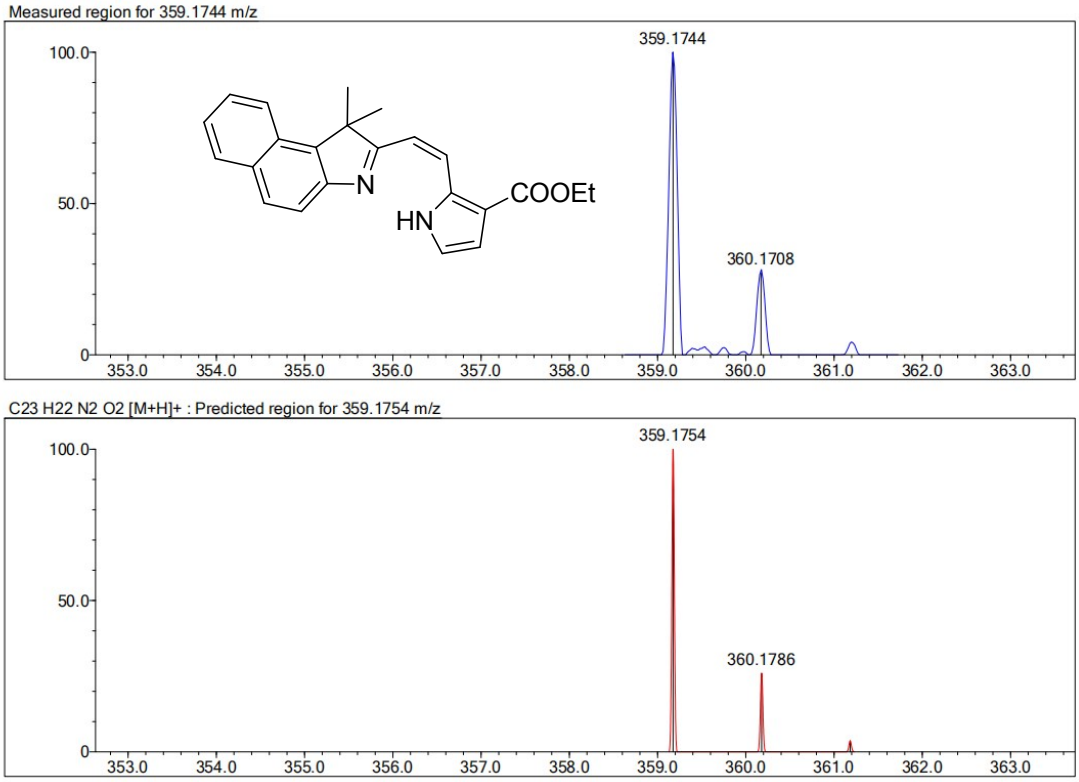

Figure S42 HRMS (ESI) spectra of **NB-3**

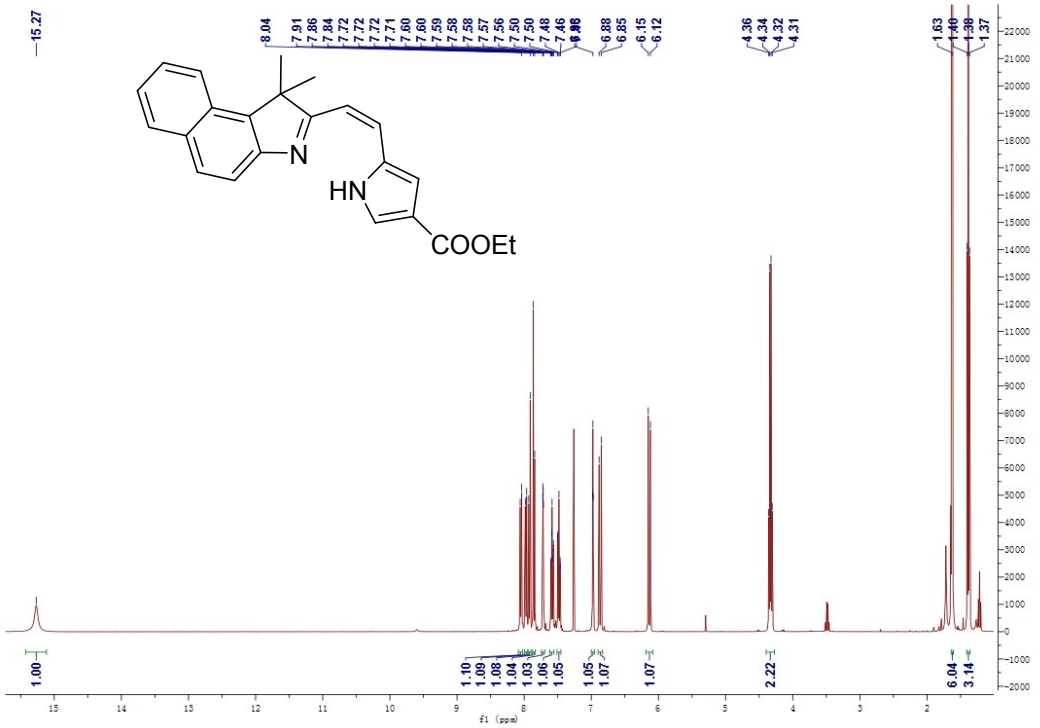

Figure S43 ^{1}H NMR spectra of **NB-4**

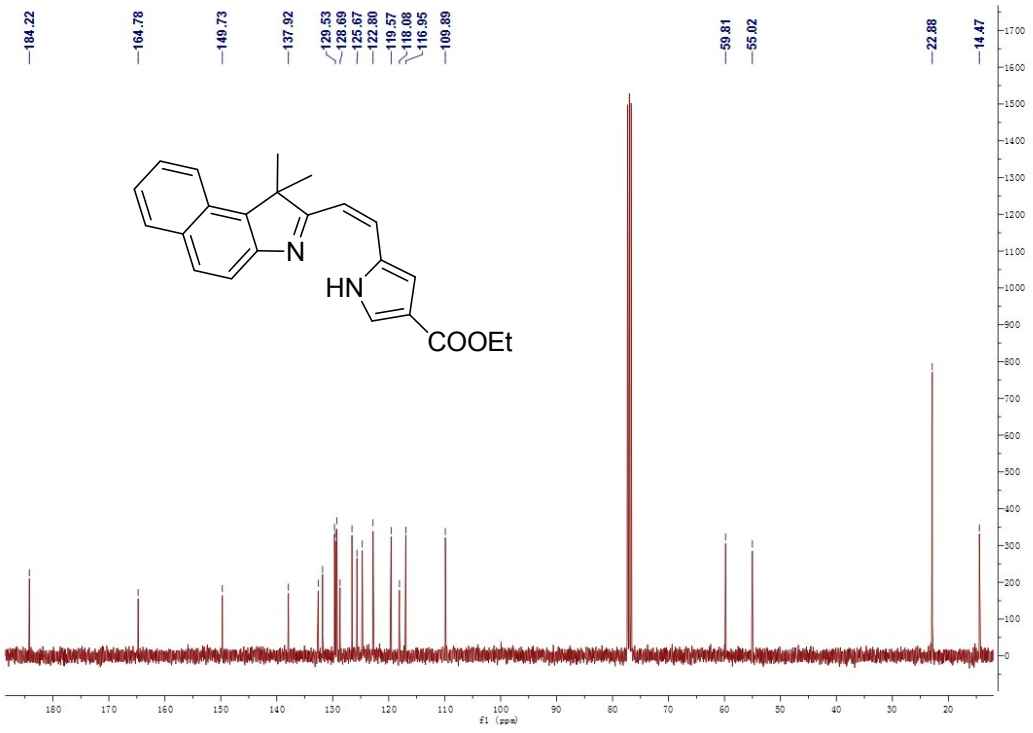

Figure S44 ^{13}C NMR spectra of **NB-4**

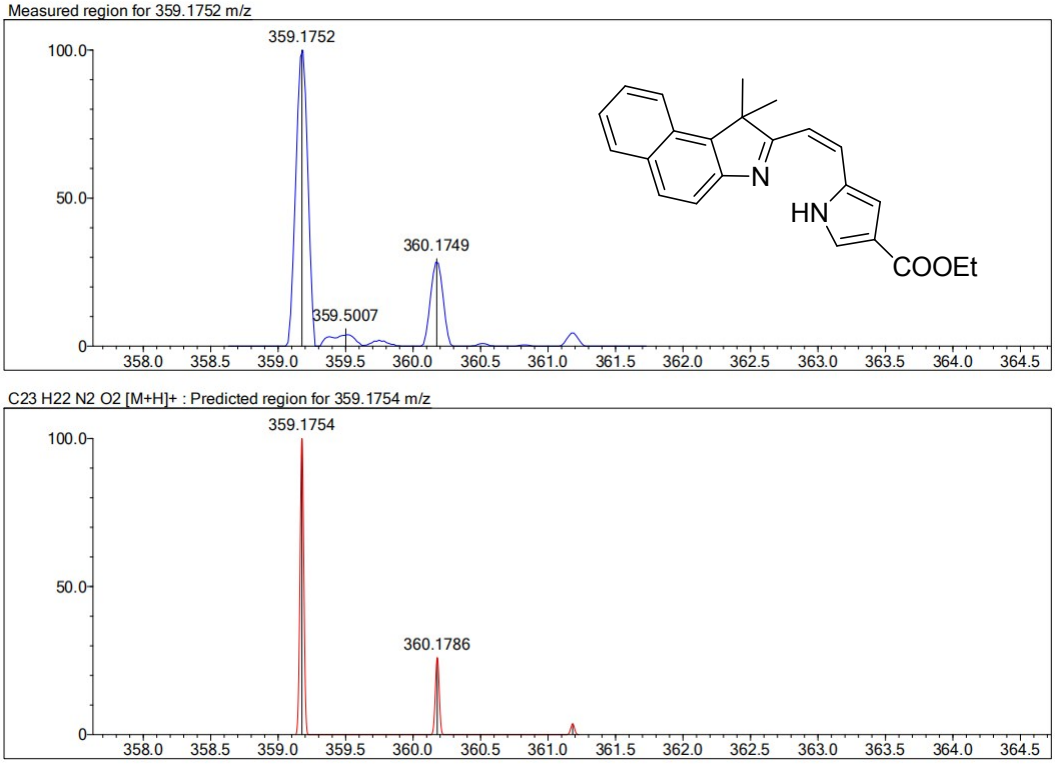

Figure S45 HRMS (ESI) spectra of **NB-4**